Advances in Fluorescence and Bioluminescence Imaging

ARTICLE *in* ANALYTICAL CHEMISTRY · NOVEMBER 2012

Impact Factor: 5.64 · DOI: 10.1021/ac3031724 · Source: PubMed

3 AUTHORS, INCLUDING:

Hideaki Yoshimura
The University of Tokyo
17 PUBLICATIONS **253** CITATIONS

SEE PROFILE

analytical chemistry

Review

pubs.acs.org/ac

Advances in Fluorescence and Bioluminescence Imaging

Takeaki Ozawa,*[,†] Hideaki Yoshimura,[†] and Sung Bae Kim[‡]

[†]Department of Chemistry, Graduate School of Science, The University of Tokyo, 7-3-1 Hongo, Bunkyo-ku, Tokyo 113-0033, Japan

[‡]Research Institute for Environmental Management Technology, National Institute of Advanced Industrial Science and Technology (AIST), 16-1 Onogawa, Tsukuba 305-8569, Japan

CONTENTS

Recent progress of bioanalytical techniques has accelerated the deep understanding of cellular states and development of novel drugs as well as medical diagnosis. Particularly, small organic molecules, quantum dots, and genetically encoded optical probes have revolutionized imaging and analysis of intracellular molecular networks during the past decade. The emphasis of this review is advancement of less-invasive imaging technologies with optical probes and their applications published in the most recent 3 years. The substantial progress is to allow for direct visualization of a wide variety of biological events in living cells and animals with higher spatiotemporal resolution. We discuss their characteristic benefits, limitations, and current challenges posed for the next generation of imaging science.

A current trend of modern science points to a deeper understanding of life phenomena that transcends the frameworks imposed by existing biological fields. Particularly, it is crucial to understand molecular network in living subjects as a system. Novel analytical techniques and methods have contributed strongly to the elucidation of many complicated biological networks. For example, comprehensive genomic analysis of higher animals was realized at the end of the 20th century, radically advancing the knowledge of correlative genes and evolving the understanding of life phenomena. The analysis has been supported strongly by capillary electrophoresis and chemical modification of oligonucleotides, which is expected to engender the next generation of DNA sequencing with higher performance. Now is a transition period to elucidate the gene products including various RNAs, proteins, lipids, sugars, and small molecules with novel technological advances.

Single-cell analysis is an intriguing target to elucidate their true nature as the smallest unit of life. Each cellular function comprises complicated networks of numerous molecules and proteins in the cells. The networks comprise sequential and parallel signal transduction events, including protein−protein interactions, enzymatic reactions, and protein modifications such as phosphorylations, methylations, and ubiquitinations. Proteomics and metabolomics analysis are now enabling the accumulation of numerous data related to biological molecules and their functions. Nevertheless, the data are typically obtained as an average over a population of cells, which sometimes obscures the actual characteristics and behavior of individual molecules. In fact, many molecular events do not occur uniformly but are instead transduced with an appropriate timing manner at a specific area. It is still difficult to investigate and analyze such spatiotemporal molecular events at the single-cell level. In addition, the absolute number of some molecules is quite low in a single cell because the volume of the cell unit is normally less than 10^{-10} L, where sometimes only countable molecules are present. Such a small number of molecules cannot be explained as a concentration but as a number of molecules. Therefore, the challenging task necessitates the use of many new technologies such as single-cell-based analyses using cell microarrays, cell chips, nanofluidics, cell patterning, and high-content analyses as well as microscopes.

To analyze the biological events in single cells, technologies related to fluorescence and luminescence imaging have been advancing rapidly in the past decade (Figure 1). Remarkable advancement has been achieved in the visualization of bioactive

Special Issue: Fundamental and Applied Reviews in Analytical Chemistry 2013

Published: November 7, 2012

   dx.doi.org/10.1021/ac3031724 | *Anal. Chem.* 2013, 85, 590−609

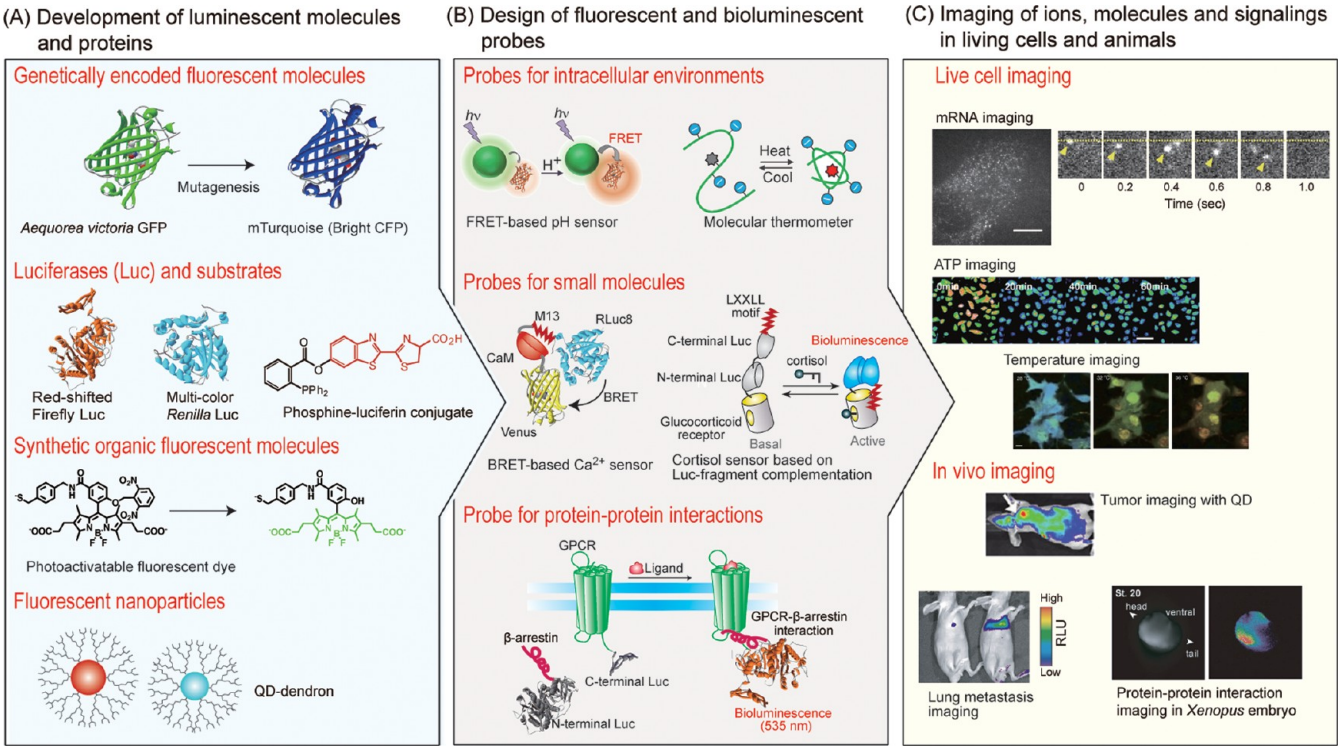

Figure 1. Advancement of fluorescence and bioluminescence imaging. Visualization of a specific molecule is achieved by three steps: development of fluorescent and bioluminescent materials (A), design and creating of the probes (B), and imaging of a specific target (C). Reprinted from ref 43. Copyright 2012 American Chemical Society. Reprinted from ref 54. Copyright 2012 American Chemical Society. Reprinted from ref 75. Copyright 2010 American Chemical Society. Reprinted with permission from ref 77. Copyright 2012 Nature Publishing Group. Reprinted from ref 95. Copyright 2011 American Chemical Society. Reprinted with permission from ref 143. Copyright 2009 Hida et al.

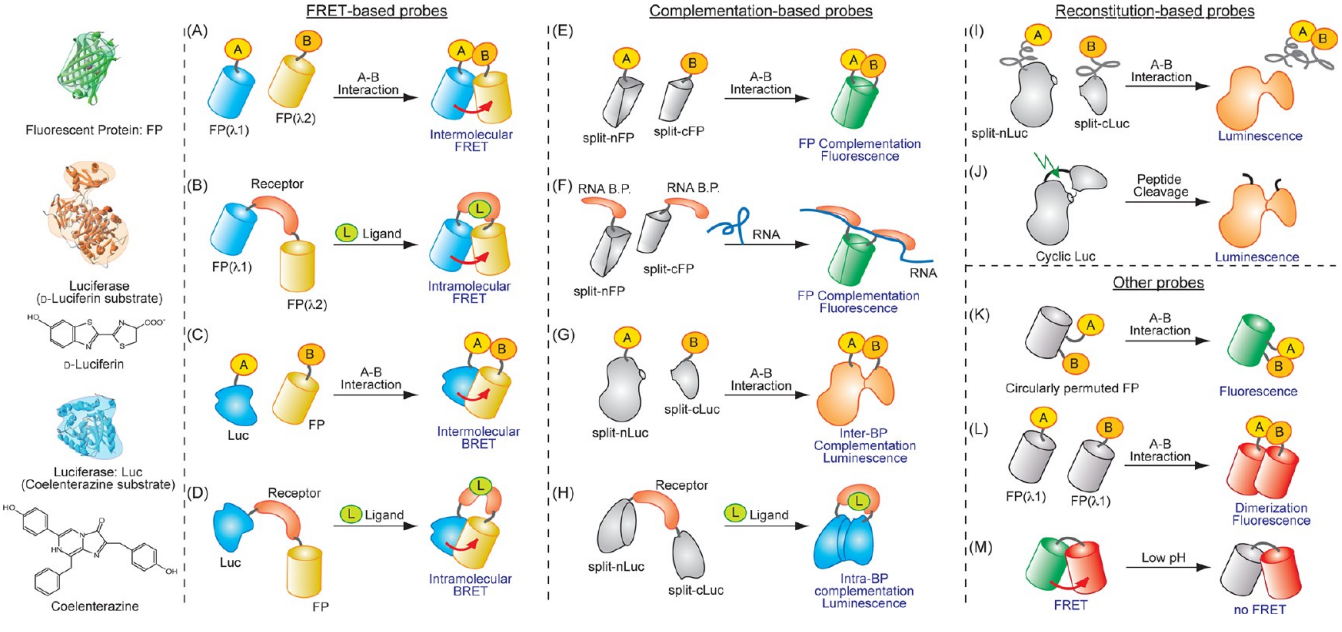

Figure 2. Representative design of fluorescent and bioluminescent probes. Structures of a fluorescent protein (FP), luciferases (Luc), and their substrates are shown in the left side. (A) Intermolecular FRET-based probe. (B) Intramolecular FRET-based probe. (C) Intermolecular BRET-based probe. (D) Intramolecular BRET-based probe. (E) A probe based on split FP-fragment complementation. nFP and cFP indicate N-terminal and C-terminal halves of FP, respectively. (F) A RNA probe based on split FP-fragment complementation. (G) A probe based on intermolecular split Luc-fragment complementation. (H) A probe based on intramolecular split Luc-fragment complementation. (I) A probe based on split Luc-fragment reconstitution. (J) Cyclic Luc probe. (K) Circularly permuted FP probe. (L) FP homodimerization-based probe. (M) pH probe based on chromophore environment.

small molecules, protein conformational changes, protein localization and dynamics, and protein−protein interactions in real-time at the level of single living cells and organisms with high spatial and temporal resolution. For example, ions and small molecules can be visualized with small fluorescent organic molecules named organic probes. The probes are now

dx.doi.org/10.1021/ac3031724 | Anal. Chem. 2013, 85, 590−609

synthesized according to rational design of fluorescent molecules. Nanoparticles represented by quantum dots are often used for single molecule analysis in live cells.[1] Although they are still larger than the organic probes or genetically encoded ones, the particles present important benefits in terms of the special character of their stability of luminescence and spectra, which has improved remarkably over the past decade. In addition, the improvement of green fluorescent protein (GFP)-like fluorescent proteins has achieved great breakthroughs in the field of molecular imaging.[2] Many efforts of researchers have been devoted to modification of the properties through genetic engineering of diversified spectra, enhanced brightness and photostability, better folding efficiency, and decreased oligomerization. In addition, the development of optical highlighters that can be controlled by irradiation with external light is widely useful for tracking a specific protein within a living cell and super-resolution fluorescence imaging.[3] These fluorescent proteins, which are photoactivatable, photoconvertible, and photoswitchable, can be switched on and off by illumination at specific wavelengths differing from the excitation wavelength. Aside from those fluorescent proteins, different bioluminescent proteins and their substrates have emerged to visualize molecular and cellular functions and disease states in animal models.

Because of the development of fluorescent and bioluminescent proteins, many strategies and molecular design enabling visualization of intracellular signaling have been realized (Figure 2). One accepted imaging strategy includes fluorescence resonance energy transfer (FRET) and bioluminescence resonance energy transfer (BRET). The FRET and BRET involve nonradiative energy transfer from a donor molecule to an acceptor one. The energy transfer occurs when the excitation spectrum of the acceptor overlaps with the emission spectrum of the donor and when the two fluorophores are close in proximity (less than 10 nm) and are in a favorable orientation permitting dipole−dipole coupling. Applicability of the FRET and BRET is classified into two-ways: intramolecular FRET (or BRET), which is often used for ion or small molecule sensing; and an intermolecular FRET (or BRET), which is applicable for imaging protein−protein interactions. Protein-fragment complementation has also been widely used for the analysis of intracellular signals.[4] For complementation analysis, fluorescent or bioluminescent proteins are rationally dissected into two nonluminescence fragments. When the fragments are brought into proximity, the fragments refold into the unique structure of fluorescent or bioluminescent proteins, which restore the luminescence. This complementation analysis provides important information related to cell signaling events such as protein−protein interaction, protein phosphorylation, and RNA localization. Protein-fragment reconstitution closely resembles complementation, but the reconstitution can be achieved by protein splicing. The protein splicing is a naturally occurring posttranslational domain rearrangement involving precise excision of an internal protein segment (named intein) from a primary translation product with concomitant ligation of the flanking peptide sequences (named extein).[5] Some specific inteins are naturally composed of two fragments mediating a trans-splicing reaction with high efficiency. When the inteins are connected with split fragments of fluorescent or bioluminescent proteins, the luminescence is recoverable after reconstitution by protein splicing. This technology is used for the analysis of protein translocation into a target intracellular organelle.[6] This reconstitution is also used for enabling peptide cyclization.[7] When the amino and carboxy ends of proteins are connected with the split intein fragments, the ends are connected by peptide bond to generate a cyclic protein, which was first applied for the analysis of protease imaging in living cells and animals.[8]

In the following section, we briefly survey recent advancement of different probes for each particular target in living cells and animals. More unique designs of fluorescent and bioluminescent probes are now generated, as emphasized in each section.

FLUORESCENCE IMAGING

Fluorescent molecules and probes are great tools for cell biologists. They have led a revolution in the field of molecular imaging over the past decade. Real-time tracking of various biomolecules and physiological events in live cells is a representative example. Furthermore, advancements have been made in fluorophore labeling technology, development of various series of fluorophores that allow for simultaneous multicolor imaging, emergence of different types of probe design, improvement of fluorescence brightness, photostability, unwanted oligomerization, environmental sensitivity, and signal-to-noise ratio, etc. Because of that innovative progress, fluorescence bioimaging has become the most widespread technique to investigate spatiotemporal dynamics of target molecules or events in living things. A unique feature of fluorescence imaging in comparison to bioluminescence imaging is its higher brightness, which enables visualization of an intriguing target with optical resolution and a millisecond time scale. No requirement of substrates or cofactors is advantageous compared to bioluminescence imaging. Therefore, fluorescence imaging is often used for the analysis of molecules and events occurring at a subcellular level and fast dynamics in living cells. In this session, we present a specific examination of the recent progress related to fluorescent molecules. Then, we deal with some design of novel probes for cellular processes such as ions, RNAs, environments, and the molecules functioning for cellular signaling, in which practical applications will be described below.

Fluorescent Molecules for Bioimaging. Fluorescent molecules are the most critical factor to investigate biological events at a molecular level. Three prominent types of fluorescent molecules have been used for bioimaging: fluorescent proteins, artificially synthesized organic dyes, and fluorescent nanoparticles. A characteristic benefit of fluorescent proteins is convenience of handling in live-cell imaging studies because they are genetically encoded and because they can be expressed easily into living cells by a conventional gene transfer. The genes encoding the fluorescent proteins can also be inserted in the genome, providing more valuable information in animal models. Artificially synthesized organic dyes generally have better fluorescent properties in brightness and photostability than those of fluorescent proteins. Additionally noteworthy is their small size, which reduces risks to perturb the functions of target molecules. Fluorescent nanoparticles present particular advantages in terms of their large stoke shift in addition to their brightness and photostability against bleaching but they are large. Fortunately, much progress has been made in that area.

Genetically Encoded Fluorescent Molecules. Fluorescence imaging was revolutionized first by the development of a calcium indicator of synthetic organic molecules in 1985.[9] Subsequently, cloning of the GFP from the jellyfish *Aequorea victoria*[10] has sparked live cell imaging through the development of a technique by which a fluorescent protein is labeled genetically with a protein of interest in living cells.[2] This technique is now leading to development of fluorescent proteins engineered with different spectral and functional properties. Moreover, properties of the

dx.doi.org/10.1021/ac3031724 | *Anal. Chem.* 2013, 85, 590−609

fluorescent proteins have been improved markedly to more accurate and sensitive signals from FRET and super-resolution imaging.[11,12] Some recent topics are explained in greater detail below.

Fluorescent Proteins Emitting Long-Wavelength Light. Near infrared fluorescent proteins have been sought for the use of *in vivo* fluorescence imaging of deep tissues because this wavelength region minimizes the absorbance of heme in hemoglobin and myoglobin, water, and lipids. Chudakov's group developed near-infrared fluorescent proteins based on the dimeric far-red fluorescent protein Katushka.[13] Previously, this group created a low-cytotoxicity Katushka variant, Katushka-9-5, which had spectral characteristics nearly identical to those of Katushka and which had minimal negative impact on bacterial growth. Accordingly, Katushka-9-5 was selected for the development of fluorescent protein variants with further red-shifted emissions. Site-direct mutagenesis and random mutagenesis enabled development of two red-shifted variants named eqFP650 and eqFP670 (eq originates from *Entacmaea quadricolor*). Actually, eqFP650 was the brightest fluorescent protein with its emission maximum above 635 nm. Furthermore, eqFP670 displayed the most red-shifted emission maximum and high photostability at that time.

Monomeric property of fluorescent proteins with longer wavelength also has a strong impact for application to deep-tissue imaging techniques. Many orange and red fluorescent proteins among the numerous homologues of GFP are either dimeric or tetrameric, which is unsuitable for applications as fusion tags to study localization, intermolecular binding, and motility dynamics of proteins of interest. Recently, a red fluorescent protein of mKate was improved drastically into a brighter variant of far-red fluorescent protein.[14] Advantageous property of the protein named mKate2 is faster maturation, acid-resistant, more photostable, and monomeric. Tsien et al. developed another monomeric far-red fluorescent protein.[15] They selected mKate as the starting point for directed evolution. Several mutageneses produced a protein with spectral properties of 600 nm excitation and 650 nm emission. This mKate variant, named Neptune, is the bright fluorescent protein with an excitation peak over 600 nm. The absorption and excitation peaks are 18 nm redder and the peak extinction coefficient are 71% larger than those of the parent mKate.

Although most fluorescent proteins used in bioimaging have similar structure and are derived from jellyfish and corals, phytochromes are included in fluorescent probes for bioimaging. Of the many phytochromes, bacterial phytochrome is a promising candidate because the fluorescent cofactor, biliverdin IXα, is abundant in all aerobic organisms as the initial intermediate in heme catabolism. At the current stage, phytochrome-based red fluorescent proteins of two types have emerged. One is a mutant of a chromophore-binding domain (CBD) in a bacterial phytochrome from *Deinococcus radiodurans* (IFP1.4), of which excitation and emission maxima are, respectively, 684 and 708 nm. The IFP1.4 express well in mammalian cells and mice with spontaneous incorporation of biliverdin. Exogenous addition of biliverdin to IFP1.4 expressing cells increased infrared fluorescence. The other is a variant of bacterial phytochrome, *Rp*Bph from the photosynthetic bacterium *Rhodopseudomonas palustris*.[16] After five rounds of mutagenesis, the brightest clone (iRFP) was isolated. It included 13 amino acid substitutions. The mutant exhibited fluorescence with excitation and emission maxima at 690 and 713 nm, respectively, which were slightly red-shifted, with 20% higher brightness than that of IFP1.4.

Fluorescent Proteins for FRET Probes. FRET techniques are widely applied in various indicators such as ions, second messengers, protein−protein interactions, and enzymatic activities. Development of fluorescent molecules that work as a FRET donor or an acceptor is crucial to generate workable biosensors. Lin et al. reported novel fluorescent proteins, Clover and mRuby2, which have the highest Förster radius among any ratiometric FRET pairs described to date.[17] Clover differs from GFP by 10 mutations of S30R, Y39N, S65G, Q69A, N105T, Y145F, M153T, V163A, I171V, and T203H and has excitation and emission maxima of 505 and 515 nm, which fall between those of EGFP and enhanced yellow fluorescent protein (EYFP). mRuby2 was developed by screening of mutants for maximal FRET in tandem fusion with the Clover. The excitation and emission maxima of mRuby2 are at 559 and 600 nm. Clover-mRuby2 pair has a Förster radius of 6.3 nm with random interfluorophore orientation, which is higher than that of any FRET pair reported in the literature. mRuby2 has a larger stokes shift those of representative FRET acceptor proteins such as YFP or mCherry, improving the separation of acceptor and donor emissions.

Most fluorescent proteins have been generated through fluorescence intensity-based screening of mutant libraries in *E. coli*. However, the fluorescence intensity of *E. coli* colonies reflects brightness, expression level, maturation efficiency, and colony thickness, which hamper efficient screening. Gadella Jr. and co-workers developed a new method to screen novel fluorescent proteins based on the fluorescence lifetime, which overcame the drawbacks of intensity-based screening.[18] Using the screening method, they developed a brightest cyan fluorescent protein (CFP) variant, mTurquoise, with the fluorescence lifetime of 3.78 ns, which is about 1 ns longer than that of the starting material, SCFP3A. In agreement with the increased lifetime, the quantum yield of mTurquoise was 0.84, which was 1.5-fold greater than that of SCFP3A. The novel protein showed single-exponential decay, which is crucial for time-resolved FRET measurement. Consequently, mTurquoise will become a good candidate for the design of FRET-based probes, which will enable quantitative analysis of biomolecules.

Subach et al. generated a new monomeric blue fluorescent protein, mTagBFP2, based on mTagBFP.[19] GFP variants emitting blue fluorescence generally suffer from moderate brightness and low chemical stability. The mTagBFP2 was 1.5-fold more photostable than parental mTagBFP under arc lamp illumination and brighter than mTagBFP because of its higher extinction coefficient. In addition, the usefulness of the mTagBFP was demonstrated as an excellent FRET donor for green fluorescent proteins such as mEmerald.

Photoactivatable Fluorescent Proteins (PA-FPs). PA-FPs are fluorescent proteins that alter their fluorescence properties upon irradiation with a specific wavelength. PA-FPs are widely applied to various microscopic techniques such as iFRAP, pulse-chase imaging, and super-resolution imaging based on the stochastic activation of fluorescence. Verkhusha et al. developed a novel PA-FP, named PSmOrange2, which is photoswitchable with blue light from an orange to a far-red form.[20] Compared to another orange-to-far-red photoconvertible variant, PSmOrange2 has a blue-shifted photoswitching action spectrum, 9-fold higher photoconversion and up to 10-fold faster photoswitching kinetics. The PSmOrange2 properties also allow efficient photoswitching with common two-photon lasers. Moreover, FRET from green fluorescent donors can convert PSmOrange2

dx.doi.org/10.1021/ac3031724 | *Anal. Chem.* 2013, 85, 590−609

from an orange to a far-red form. PSmOrange2 is the first fluorescent protein with photoswitching that is substantially accelerated by a FRET process from the green emitting donor.

A representative photoconvertible protein of mEos2 is widely used for super-resolution microscopy. An issue of the protein is the formation of oligomer in its high concentrations. To improve oligomerization, several mutations were inserted based on crystal structural information of mEos2 tetramer, which suggests that three key residues, I102, Y121, and Y189, might participate in the oligomerization of mEos2.[21] Two variants of mEos2 named mEos3.1 and mEos3.2, which have I102N, I157V, H158E, Y189A, and I102N, H158E, and Y189A mutations, respectively, were both truly monomeric, brighter, with faster maturation, and with a higher photon budget. Similarly, another PA-FP named IrisFP was improved into a monomeric form. IrisFP combines irreversible photoconversion from a green-emitting to a red-emitting form with reversible photoswitching between fluorescent and nonfluorescent states. This feature permits the combination of pulse-chase experiments with photoactivation localization microscopy (PALM) imaging. The spectroscopic properties, photoswitching, and thermal relaxation behavior of mIrisFP resembled those of IrisFP. The dual photoactivation capability of mIrisFP offers enhanced applicability and also enables the combination of pulse-chase experiments with super-resolution imaging.

Although many PA-FPs are irreversible, Verkhusha and co-workers developed a reversibly photoswitchable red fluorescent protein: rsTagRFP.[22] Illumination with blue light and yellow light, respectively, switches rsTagRFP into a red fluorescent state and a nonfluorescent state. Compared to the available monomeric red reversibly photoswitchable fluorescent proteins, rsTagRFP showed a substantially greater brightness and higher contrast that is independent of the switching cycle. Moreover, a dynamic absorption change that accompanies rsTagRFP photoconversion allowed for its application in photochromic FRET (pcFRET) with EYFP as a donor. The rsTagRFP-EYFP pair demonstrated a high potential of the pcFRET imaging to study subcellular protein interactions.

The Hell and Jakobs groups generated another reversibly switchable enhanced GFP, rsEGFP.[23] rsEGFP can be switched on at 405 nm and off at 491 nm light irradiation. Absorption at 491 nm yields fluorescence peaking at 510 nm and, in a competing process, switches rsEGFP off. The prominent feature of rsEGFP is that this can be photoswitched reversibly more than a thousand times. The reversible switching also enables all-optical writing of features with subdiffraction size and spacing, which is useful for data storage. The group also reported a bright, monomeric, reversibly photoswitchable variant of GFP, named Dreiklang, of which the fluorescence excitation spectrum is decoupled from that for optical switching.[24] Reversible on-and-off switching is accomplished at ∼365 and ∼405 nm light irradiation, respectively, and fluorescence emission takes place by excitation with ∼515 nm light. Dreiklang enables fine-tuning of the duration of the chromophore states without interference by the fluorescence excitation light. This feature provides benefits for super-resolution microscopy applying stochastic single-molecule switching and spatial target switching.

Fluorescent Timers. Fluorescent proteins that change their emission wavelengths over time, called fluorescent timers, are valuable to visualize temporal and spatial molecular events such as protein homeostases. Fluorescent timers have also facilitated the investigation of cellular fate and its related diseases. Verkhusha and Pletnev developed three mCherry-derived monomeric variants, called fluorescent timers (FT), which change their fluorescence from blue to red over time.[25] In fact, FTs have been generated through multiple saturated mutagenesis of mCherry, resulting in fast-FT, medium-FT, and slow-FT. These FT variants exhibited distinctive blue-to-red chromophore maturation rates. The maxima of the blue fluorescence were evaluated at 0.25, 1.2, 9.8 h, and the half-maxima of the red fluorescence reached at 7.1, 3.9, and 28 h, respectively, for the purified fast-FT, medium-FT, and slow-FT. Structural analysis has suggested that the blue-to-red conversion is associated with the oxidation of the Cα2—Cβ2 bond of Tyr67.[26]

In contrast to the monomeric timer proteins, the group of Schiebel and Knop developed a tandem fluorescent protein timers, tFTs.[27] tFTs were generated from mCherry and superfolder GFP (sfGFP). mCherry matures with a half-time of about 40 min, whereas sfGFP becomes fluorescent within minutes. This tFT mostly emits green fluorescence shortly after synthesis; it then acquires red fluorescence gradually over time. The mCherry-sfGFP is so bright that it enables the measurement of turnover, mobility, and inheritance of endogenously expressed protein fusions in living cells on time scales from ∼10 min to several hours.

Other Genetically Encoded Proteins and Their Applications. Campbell's group developed a novel design of fluorescent proteins named dimerization-dependent red fluorescent protein (ddRFP), which emits fluorescence only when the protein forms a dimer.[28] Many red fluorescent proteins take oligomeric structures. The structures stabilize the chromophore in conformations that favor bright fluorescence. The group attempted to develop an alternative biosensing system by engineering the oligomeric structure of RFPs to create a low affinity heterodimer that exhibited bright red fluorescence in the associated state and dim fluorescence in the dissociated one. To generate a fluorogenic RFP heterodimer, a monomeric and dimly fluorescent RFP variant was created by introducing the H162K and A164R substitutions into a representative red fluorescent protein: dTomato. Then a dTomato-derived partner was created to set out to "rescue" dimer formation and fluorescence with surface modifications that complemented the modifications to the first dTomato mutant. The ddRFP pair, A1 and B1, selected through several rounds of screening, exhibited a 10-fold increase in fluorescence upon dimerization with K_d of 33 μM. Applicability of this ddRFP was shown for detection of protein−protein interactions *in vitro*, imaging of the reversible Ca^{2+}-dependent association of calmodulin (CaM) and M13 in live cells, and imaging of caspase-3 activity during apoptosis.

Approaches that exploit a single-excitation wavelength for multiple fluorescent probes with resolvable emission spectra are of special interest. Recently, a new orange fluorescent protein with a large stokes shift (excitation/emission at 437/572 nm) has been reported.[29] The protein, LSSmOrange, was applied for simultaneous imaging of two FRET pairs with a single excitation light. In this experiment, a caspase activity and Ca^{2+} was simultaneously monitored, respectively, with FRET pairs of LSSmOrange-mKates and CFP-YFP. Both FRET donors were excited efficiently with a single wavelength of 440 nm, whereas the emission of the LSSmOrange-mKate2 pair was resolvable spectrally from that of the CFP-YFP pair. Consequently, LSSmOrange allowed for multicolor applications using single-wavelength excitation. The properties of LSSmOrange are expected to broaden the applicability of simultaneous multicolor

dx.doi.org/10.1021/ac3031724 | *Anal. Chem.* 2013, 85, 590−609

imaging to track and quantify multiple populations of intracellular objects.

Synthetic Organic Fluorescent Molecules for Bioimaging. Small artificial organic molecules typically have excellent properties such as small molecular weight, a variety of fluorescence wavelength, brightness, and stability against photobleaching, in comparison to fluorescent proteins. Recently, photochromic properties such as PA-FPs have been shown for organic fluorescent molecules. One example is the generation of photoactivatable and photoconvertible fluorescent probes that can be coupled selectively to SNAP-tag fusion proteins in living cells.[30] The photosensitivity of the probes is based on the photocleavage of a linker between a quencher or a second fluorophore and the fluorophore of interest. The probe molecules contain a benzylguanine moiety for attachment to SNAP-tag fusion proteins, and fluorescein and Cy3 for photoactivatable versions, or Cy5 and Cy3 for photoconvertible versions. This study established a generally applicable strategy for the generation of energy transfer-based photoactivatable and photoconvertible organic probes that can be attached to SNAP-tag fusion protein in living cells. Urano and co-workers presented a novel design for a new class of caged BODIPY fluorophores using photoremovable protecting groups.[31] This caged fluorophore was efficiently photoactivated, with 600-fold increases in the fluorescence intensity. This photoactivatable fluorophore, which was combined with a SNAP ligand to attach SNAP-tag fusion proteins, demonstrated spatiotemporal imaging of the epidermal growth factor receptor in living cells.

An important difficulty related to the application of organic fluorescent molecules to cellular imaging is the targeting in (or on) an intracellular compartment. Artificially synthesized fluorophores are usually labeled to a target molecule through conjugation to antibodies or tag proteins such as SNAP-tag. In the labeling process, nonspecific binding of the fluorophores is unavoidable even with washing out after staining. A technique of a fluorescence activation-coupled protein labeling method overcame this problem: only the fluorescent molecules attached to the cognate tag proteins emitted fluorescence.[32,33] The probe contained a fluorophore and a quencher and exhibited almost no basal fluorescence. Upon binding to tag proteins, the quencher portion was removed. Only the fluorophore was attached to the tag, acquiring strong fluorescence. Consequently, this method enabled real-time imaging of protein labeling without the need for a washout process to remove excess probes.

RNA aptamers are applicable as new chemical probes. The aptamers developed by Jaffrey's group bind fluorophores resembling the GFP fluorophore of 4-hydroxybenzlidene imidazolinone (HBI).[34] Naked GFP fluorophore is nonfluorescent, but it recovers its fluorescence after GFP refolding. An RNA sequence with GFP-like properties might exhibit fluorescence upon binding a small-molecule fluorophore. On the basis of this idea, the group developed several combinations of HBI derivatives and RNA aptamers. Although an HBI derivative itself was detectably nonfluorescent in the presence of cellular RNA or DNA, the derivative and a particular RNA aptamer, termed Spinach, emitted green fluorescence, comparable in brightness with fluorescent proteins. The variety of RNA-HBI derivative complexes created a palette that spans the visible spectrum. Spinach enabled imaging of RNAs in living cells. In addition, modified Spinach allowed for a sensor for small molecules by the insertion of an aptamer sensor for the target.[35] The applicability was demonstrated for adenosine, ADP, SAM, guanine, and GTP, which were detected, respectively, through 20-, 20-, 25-, 32-, and 15-fold fluorescence increases. The ability to confer GFP-like functionality to RNA is expected to facilitate studies of RNA biology and advanced RNA-based applications.

Fluorescent Nanoparticles for Bioimaging Studies. Nanoparticle-based tags can bring great benefits for *in vivo* and therapeutic imaging because of their brightness and stability of the fluorescence.[36] Nanoparticles are categorized according to their properties such as nanocrystals of semiconductors, metal nanoclusters, and organic polymer nanobeads. Successful conjugation of biomolecules onto nanoparticles depends strongly on appropriate surface modification.[1] A robust method to conjugate semiconductor quantum dots (QDs) with cognate partners such as antibodies was reported by Weiss et al.[37] The QDs of CdSe/CdS/ZnS were coated with glycine or lysine N-terminated peptides, causing the peptide coated QDs, which reacted with pentafluorophenyl-poly(ethyleneglycol)-4-formylbenzamide (PF-PEG-FB). However, antibodies were modified with succinimidyl-6-hydrazinonicotinate acetone hydrazone (NHS-HyNic). Then the modified QDs and antibodies were coupled to generate antibody-conjugated QDs.

In addition to difficulties of successful conjugation of nanoparticles to the target biomolecules, nonspecific binding, difficulty of intracellular delivery, and endosomal trapping are crucial reasons to hamper specific target binding in live cells. To reduce these problems, polymer-coated QDs (pcQDs) of which surfaces were optimized for specific intracellular targeting were generated.[38] In the modification process, the surface of pcQDs was initially covered with polyethylene glycol (PEG) to allow for efficient intracellular delivery. Then, the elimination of marked endosomal sequestration of the QDs was achieved through the conjugation of a cell penetrating peptide: TAT. On the basis of this principle, Choi et al. presented antibody-functionalized TAT-PEG-pcQDs.[38] To demonstrate the intracellular targeting specificity of this QD conjugate, a model cell line overexpressing GFP-tagged endothelin A receptor (ET_AR) in its cytoplasm was constructed. In fluorescence-imaging experiments, the anti-GFP antibody-functionalized TAT-PEG-conjugated QDs strongly colocalized with GFP-ET_AR. This result indicated the ability of the functionalized QDs to penetrate the cell membrane and to attach selectively to GFP. Consequently, PEG-pcQDs conjugation with cell penetrating peptide and an antibody against a target biomolecule will allow specific binding to a target with minimized nonspecific binding.

Despite the various modifications of QDs, large physical diameters, strong fluorescence blinking, and toxic elements of QDs compromise their widespread application. In this respect, fluorescent metal nanoclusters are attractive for use in biosensing and bioimaging because of their subnanometer size as well as excellent photostability and low toxicity. Particularly, silver nanoclusters prepared using cytosine-rich single-stranded DNA templates have attracted special attention because of their facile synthesis.[39] Zhu et al. developed a method to functionalize oligonucleotide-templated silver nanoclusters (Ag NCs) with a oligonucleotide aptamer through a facile one-pot process.[40] In this study, AS1411, an oligonucleotide aptamer to nucleolin, was rationally connected with polycytosine via a TTTTT loop (T5 loop). It was used as the scaffold to synthesize Ag NCs through a one-step process. Prepared Ag NCs functionalized with AS1411 were internalized into MCF-7 cells and were able to stain the nuclei specifically with a red color. The binding affinity of the Ag NCs to nucleolin provided opportunities for the application in intracellular imaging and nuclear staining.

dx.doi.org/10.1021/ac3031724 | *Anal. Chem.* 2013, 85, 590−609

Unlike QDs and metal nanoclusters, polymer particles such as polystyrene beads do not emit fluorescence by themselves. Fluorescence polymer beads are generally prepared by doping organic synthesized fluorophores into polymer particles. This method allows for creating fluorescent particles with widely various fluorescent properties depending on the doped fluorophores. In addition, the stability of fluorescence is better than those of solvent-exposed organic fluorophores because of caged effects. As an example, polystyrene nanoparticles (PS-NPs) doped with an oxygen-sensitive near IR emissive palladium complex were reported.[41] In oxygen-sensing nanoparticles, an inert dye, DY-635, was also doped as the reference. Both the oxygen sensitive dye and the reference dye were excited with a 635 nm laser. Then the emissions were separated using optical filters. In a high-oxygen concentration condition, the palladium dye emitted low fluorescence, although the fluorescence intensity of the dye became stronger at a low oxygen concentration. This property led to ratiometric fluorescence sensing for oxygen.

Silica nanoparticles are also good candidates for the preparation of fluorescent nanoparticles including fluorescent dyes.[42] In the study, tris(2,2-bipyridyl)dichlororuthenium(II) hexahydrate (Rubpy) and methylene blue (MB), which functions as a FRET pair, were doped into silica nanoparticles. The energy transfer from Rubpy to MB caused a near-infrared fluorescence with strong fluorescence intensity and a large Stokes shift (>200 nm). Because of the large Stokes shift, excellent photostability, and NIR spectral properties, the new silica nanoparticles are expected to enable real-time deep-tissue fluorescent imaging of live animals.

Spectral features of fluorescent nanoparticles, particularly strong fluorescence intensity even in near-infrared (NIR) emissions, realize many *in vivo* imaging experiments. Biocompatible Dendron-coated NIR QDs (QD-Dendron) were applied to *in vivo* tumor imaging caused by their high stability in biological media, suitable size with possible renal clearance, and ability of extravasation.[43] The QD-Dendrons were conjugated to arginine−glycine−aspartic acid peptide dimers (RGD_2). This functionalized QD (QD-Dendron-RGD_2) specifically accumulated to integrin $\alpha_v\beta_3$-positive tumor cells, enabling *in vivo* fluorescence imaging to detect tumors in mice. The probe will be applied for detection of different desired targets if QD-Dendron conjugates other disease-specific biomolecules for targeting.

In spite of the many benefits of QDs for *in vivo* imaging, their use in therapeutic experiments is limited because of the intrinsic toxicity that might cause risks to humans. Metal clusters, particularly gold and silver, offer great potential for application in biomedicine because of their inert reactivity. On the basis of this knowledge, fluorescent properties and biocompatibility were investigated to explore the application for *in vivo* imaging.[44] Fluorescence gold nanoclusters were introduced into a murine hindlimb ischemic model to evaluate the tracking and angiogenic potential of human endothelial progenitor cells. Human endothelial progenitor cells harboring the fluorescence gold nanoclusters were introduced into a murine hindlimb ischemic model to evaluate the tracking and angiogenic potential of the cells. Regarding fluorescent properties of the clusters, red emissions of the cluster showed good transparency and were distinguishable from green autofluorescence from tissues in ischemic organs. A wider application of fluorescent gold nanoparticles can be achieved with conjugation to peptides, specific antibodies, and functional molecules.

Fluorescent Probes for Biological Events. Aside from improvement of fluorescent proteins and molecules in themselves described above, novel design of different fluorescent probes has been constructed extensively. Imaging taken with the probes provides valuable information related to spatiotemporal properties of molecular distributions, enzymatic activities, intracellular environments, and so on. In this section, we discuss the novel design of the probes and their applied technique to visualize a specific target in living cells and animals.

Probes for RNAs. Increasing interest has arisen in dynamics and localization of RNAs in organisms and cells. Subcellular localization of mRNAs has recently been shown to have physiological functions. Moreover, numerous noncoding RNAs have been discovered, although their function remains somewhat of a mystery. Therefore, RNAs are now attractive targets for the studies in biological and medical fields. To visualize RNAs in cells and organisms, molecules that specifically recognize the target RNA are necessary. A most useful approach for RNA visualization at the present stage is the fluorescence *in situ* hybridization (FISH), where fluorescence-labeled oligonucleotide that has a complementary sequence to the target RNA introduced into chemically fixed samples. The fixation limits applicable to bioimaging because the probe oligonucleotides must be washed out after staining to eliminate background fluorescence. Therefore the sample must be permeable and fixed cells or tissues. Therefore, novel methods to label specific RNAs in living samples have been eagerly sought.[45,46]

Okamoto's group developed a tag technology for RNA imaging in living cells based on unique chemical functions of exciton-controlled hybridization-sensitive oligonucleotide (ECHO) probes.[47] Repeats of selected 18-RNA sequences were incorporated into the 3′-UTR of the mRNA of interest as a tag moiety. Pairs with complementary ECHO probes emitted fluorescence upon hybridization with the tag in the target mRNA in living cells. Hybridization of the ECHO probes with the complementary strand in the tag attached to the target RNA showed a strong emission because dissociation of aggregated dyes by hybridization with the complementary nucleic acid caused the disruption of excitonic interaction. Another approach developed by Kummer et al. is the hybridization-sensitive oligonucleotide probe that requires no artificial tag sequences in the target mRNA.[48] The probes, so-called FIT-PNA probes, contained a single thiazol orange intercalator serving as an artificial fluorescent nucleobase. These probes responded to changes of the local structure near the dye rather than to the more global changes of conformation. Live cell imaging of mRNA from an influenza virus strain was demonstrated using the FIT-PNA technique.

A new in situ RNA imaging method with single-molecule sensitivity was reported by Tyagi and co-workers to define the intracellular sites of RNA splicing.[49] The methods involved the attachment of multiple fluorophores to target mRNAs via hybridization probes, which rendered them so intensely fluorescent that each molecule was regarded as a diffraction-limited spot using a wide-field microscope. A pair of distinctly labeled probe sets, one against the coding sequence and the other against an intron, enabled visualization of spliced mRNA molecules in one fluorophore and the free introns in the other. In addition, the pre-mRNA molecules were visible in both fluorophores. This method enables us to view the precursor and product of splicing with single-molecule sensitivity.

Genetically encoded probes provide valuable information because the gene can be inserted in the genome of model animals. The probes are generally designed to consist of an RNA-binding protein and a fluorescent one. A coat protein of

dx.doi.org/10.1021/ac3031724 | *Anal. Chem.* 2013, 85, 590−609

bacteriophage MS2, which binds to a unique hairpin in the phage genomic RNA with a strong affinity was identified as an ideal tag. Singer et al. generated a stable cell line from transgenic mouse, where all β-actin mRNA was labeled with a MS2-YFP fusion protein.[50] Using MS2-YFP, β-actin mRNA molecules that were modified with multiple MS2 tags were visualized in their undisturbed native environment. Combining electron multiplying (EM) CCD cameras with this labeling method, observation was made with a time resolution of 20 ms. In addition, a knock-in mouse line with an MS2 binding site cassette targeted to the 3′ untranslated region of the β-actin gene was generated.[51] That line is expected to be useful for studies of endogenous mRNA regulation in any tissue or cell type.

Ozawa et al. adopted a different approach to generate a genetically encoded mRNA probe.[52] The probe used an RNA binding protein, Pumilio homology domain (PUM-HD) of human Pumilio1, with reconstitution of split fragments of enhanced GFP (EGFP). Using this technique, his group succeeded in single-molecule visualization of nonengineered endogenous β-actin mRNA in living cells (Figure 3).[53,54] In these

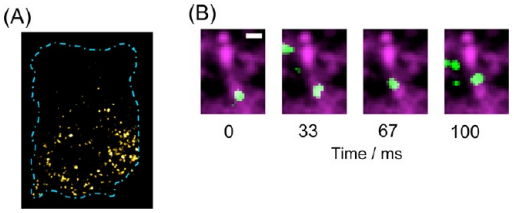

Figure 3. Imaging of β-actin mRNA using split fluorescent protein complementation. The basic principle is shown in Figure 2F. (A) Localization of β-actin mRNA distributed in the living NIH3T3 cell. Yellow dots represent β-actin mRNAs. The blue dotted line indicates the edge of the cell. (B) Single-molecule tracking of β-actin mRNA. Single β-actin mRNAs are shown in green overlaid with microtubules (purple).

reports, two PUM-HD mutants that recognize two 8-based sequences in the 3′ UTR region of β-actin mRNA were connected, respectively, with N-terminal and C-terminal fragments of EGFP. Upon probe binding to β-actin mRNA, the EGFP fragments are reconstituted, and the fluorescence is recovered. Using this probe combining total internal reflection fluorescence (TIRF) microscopy, single-molecule visualization of nonengineered endogenous β-actin mRNA in living cells was demonstrated. The similar β-actin mRNA probe was also reported, where the probe consists of two PUM-HD mutants and a full-length GFP and also allowed for single-molecule visualization of nonengineered endogenous β-actin mRNA in living cells.

Tilsner et al. applied the method using PUM-HD mutants to visualize the genomic RNA of tobacco mosaic virus (TMV) in living plant cells.[55] Two PUM-HDs, fused to either the N-terminal or C-terminal half of split mCitrine, were engineered to recognize two closely adjacent 8-base sequences in the TMV genomic RNA. Binding of the PUM-HDs to the target sites brought the split mCitrine moieties into proximity, resulting in complementation occurring and revealing the localization of viral RNA in infected cells.

Probes for Kinase Activity. Protein kinases with activity that is restricted in space and time are important regulators in living cells. A general strategy to visualize a kinase activity is to detect FRET efficiency caused by a probe conformational change. A general design of the indicators comprises a substrate domain and a docking domain flanking with two fluorescent proteins as the FRET donor and acceptor in a unique order. When a kinase is activated, the substrate region is phosphorylated, resulting in binding of the docking domain to the phosphorylated substrate. Consequently, two fluorophores come close to each other and FRET occurs. Using this principle, a probe for Jun N-terminal kinase (JNK) activity in living cells was developed recently.[56] This probe included ECFP and a citrine, respectively, as the FRET donor and acceptor. FHA1 paired with JDP2 phosphorylation site was linked to its docking domain, which was sandwiched between the ECFP and citrine. Activated JNK phosphorylated JDP2, then FHA1 interacted with JDP2, accompanied by increasing FRET efficiency between the two fluorescent proteins. The same design was adopted for development of a FRET biosensor specific for CyclinB1-Cdk1 based on the same principle.[57] In this biosensor, mCerulean and YPet were used as the FRET pair, and a polo box domain of Plk1that bind the CDK phosphorylation site was used as the phospho-binding domain. Using this probe, CyclinB1-Cdk1 was revealed to be inactive in the G2 phase and activated at a set time before nuclear envelope breakdown.

The linker design of the FRET-based probes influences the FRET efficiency. Matsuda and co-workers produced a new technique to design FRET biosensors using long flexible linkers ranging from 116 to 244 amino acids long.[58] The key concept is to exclude the orientation-dependent FRET and to make the biosensors only distance-dependent. This long linker reduced the background energy transfer and increased the gain of the FRET biosensors. This technique improved FRET efficiencies for previously reported FRET biosensors: PKA, ERK, JNK, EGFR/Abl, Ras, and Rac1.

An approach that is completely different from the FRET-based probe was reported.[59] In this study, monobodies are used as scaffolds to detect kinase activity. A library of fibronectin monobodies was screened to find a library member with the appropriate binding selectivity and affinity for the kinase of interest (Figure 4). The appropriate library member is fused to an environmentally sensitive fluorescent dye and a fluorescent protein. Probe binding to the target engenders increased fluorescence from the environmentally sensitive dye. The ratio of the dye fluorescence and that from the fluorescent protein provides a quantitative measure of the kinase activity. One of the kinases, Src family kinase (SFK), was applied with this probe, in which a monobody 1F11 is used for specific binding to an open form SH3 domain of SFKs. When the probe was bound to active SFKs, the SH3 domain took an open form, leading to increases in fluorescence. The ratio of the dye fluorescence over a protein one provided a quantitative and spatiotemporal measurement of SFK activation.

Probes for Ions, Small Molecules, and Intracellular Environments. Ca^{2+} Sensors. Local concentration of Ca^{2+} in single living cells is now an intriguing target in basic biology. An advantage of the use of genetically encoded Ca^{2+} probes is to target them on a particular organelle or on a membrane of interest in a living cell. Of the genetically encoded Ca^{2+} probes reported to date, a representative is GCaMP, which consists of circularly permuted EGFP (cpEGFP), CaM, and its binding peptide (M13).[60] The probe is designed to respond to the fluorescence intensity so large that it enables monitoring of a little change of intracellular Ca^{2+} concentration. The original GCaMP has been improved in a few years to monitor local cell signaling in live cells and mammals.[61]

The GCaMP is recently applied to monitor an intracellular Ca^{2+} concentration change in neurons. Lagnado et al. generated

dx.doi.org/10.1021/ac3031724 | *Anal. Chem.* 2013, 85, 590−609

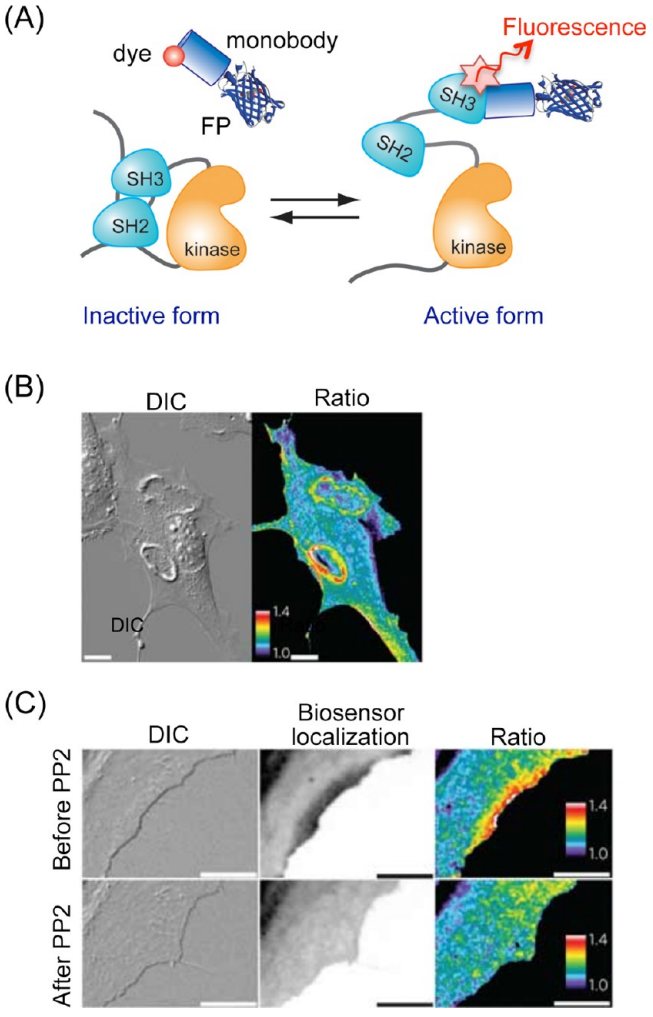

Figure 4. Biosensor for Src family kinases (SFKs): (A) basic principle of the sensor. The SFKs take an open form upon its activation, and the biosensor can bind to an exposed SH3 region. The environmentally sensitive dye on the monobody emits fluorescence after binding to the SH3 domain. Fluorescent protein (FP) emits fluorescence irrespective of binding to the SH3 domain. The fluorescence ratio of the dye to the FP indicates activity of the target SFK. (B) Differential interference contrast (DIC) image (left) and fluorescence ratio (dye/FP) image of a PDGF-stimulated NIH3T3 cell harboring the SFK biosensor (right). Scale bar, 20 μm. (C) DIC (left), the fluorescence of only FP on the biosensor (middle), and fluorescence ratio (dye/FP) images (right) of a PTK1 cell before and after Src inhibitor, PP2, treatment. Scale bar, 10 μm. Reprinted from ref 59. Copyright 2011 Nature Publishing Group.

SyGCaMP2, a fusion of GCaMP2 with the cytosolic side of synaptophysin, which is a transmembrane protein localized in synaptic vesicles.[62] Using SyGCaMP2, calcium influx was detected in parallel to the electrical activity of neurons. In addition, some applications to zebrafish neurons were demonstrated. Another but a similar GCaMP-based sensor to monitor Ca^{2+} signals in astrocytes was reported. In this report, a membrane-tethering domain, LcK, was connected to GCaMP2 and measured calcium signals near plasma membrane.[63] Furthermore, LcK-GCaMP2 was used to identify highly localized and frequent spontaneous Ca^{2+} signaling in astrocyte somata and processes, which conventional GCaMP2 failed to detect. Nakai and Kawakami improved GCaMP into more sensitive one, GCaMP-HS (GCaMP-hyper sensitive), in which the cpEGFP portion has five amino acid mutations to increase the folding efficiency.[64] The HEK293 cells transfected with GCaMP-HS gene showed 1.7-fold higher fluorescence signals than those of GCaMP2. *In vivo* Ca^{2+} imaging of neuronal activities was conducted in zebrafish larvae, demonstrating that GCaMP-HS can detect Ca^{2+} signals in both the cell bodies and neurons. Looger et al. made a modification of GCaMP2, named GCaMP3, which showed 3-fold increases in the dynamic range and 1.3-fold higher affinity for Ca^{2+}.[65] Using specific viral and promoter constructs to drive expression of GCaMP3, five major neuron classes in the adult mouse retina were labeled.[66] Stimulus-evoked GCaMP3 responses as imaged by two-photon microscopy permitted functional cell type annotation. Optical recordings from somas, dendrites, and presynaptic terminals of neurons types across the retina demonstrated the potential applicability of GCaMP3 as a tool for mapping retinal circuits.

Color variations of the Ca^{2+} sensors might uncover spatiotemporal Ca^{2+} patterns in different intracellular compartment in single cells. Campbell developed blue, green, and red intentiometric indicators through further modification of GCaMP3.[67] The produced blue variant, B-GECO1, has a 700% signal change and a K_d of 480 nM, whereas a red variant of GECO, named R-GECO1, has a 1600% intensity change and ~80 nm red-shifted absorption and emission maxima relative to the G-GECO series. Further improvement of R-GECO1 was performed by another group, and the constructed variant, R-GCaMP1.07 indicated a Ca^{2+} dependent fluorescence change that is about 2-fold greater than that of R-GECO1.[68]

Another line of genetically encoded Ca^{2+} probes is based on the FRET technique. Miyawaki et al. first developed a genetically encoded fluorescent indicator for Ca^{2+} based on GFP variants and CaM, named cameleons.[69] Yellow cameleons (YCs) have CFP and YFP, respectively, at the FRET donor and acceptor. CaM, a glycylglycine linker, and the CaM binding peptide M13 are positioned between the two fluorescent proteins. Nagai and Miyawaki then optimized the relative orientation of the two chromophores in YCs by fusing YFP at different angles using a circularly permuted technique.[70] Furthermore, Nagai's group recently reported an ultrasensitive Ca^{2+} indicator, yellow cameleon-Nano (YC-Nano), developed by engineering the Ca^{2+} sensing domain of YC variants.[71] YC-Nano ultrasensitive Ca^{2+} indicators showed affinities for Ca^{2+} of 15−140 nM and larger signal changes (1 450%). These properties enabled detection of the subtle Ca^{2+} transients associated with spontaneous network activity and reveal cell-type-dependent and stimulation dependent differences in both the resting Ca^{2+} level and the amplitude of Ca^{2+} transients.

Aside from the genetically encoded indicators, many synthetic organic probes for Ca^{2+} have been developed. These synthetic Ca^{2+} probes have some limitations such as unwanted intracellular compartmentalization, selectivity to target ions, and leakage from the cytosol to the extracellular medium. To solve these problems, a nanoparticle-based Ca^{2+} indicator was developed for quantitative imaging of intracellular Ca^{2+} ions.[72] This indicator comprises a nanoparticle loaded with rhodamine-based Ca^{2+} sensing dye, rhod2, and conjugated with Hylite Fluor 647 as the reference, those of which were encapsulated in porous and inert polyacrylamide nanoparticles. Stable signals in a range around neutral pH (pH 6−9) and sensitivity with 293 nM of K_d match the intracellular environment.

ATP Sensors. ATP is the general energy currency of all living organisms. Therefore ATP levels and distributions in living cells are crucial targets for real time bioimaging. A novel genetically encoded ATP indicator was developed based on FRET.[73] A

dx.doi.org/10.1021/ac3031724 | *Anal. Chem.* 2013, 85, 590−609

series of ATP indicators, named ATeams, comprise the ε subunit of the bacterial F_0F_1-ATP synthase sandwiched by CFP and YFP. In the ATP-free form, extended and flexible conformation of the ε subunit separate the two fluorescent proteins, resulting in low FRET efficiency. In the ATP-bound form, the ε subunit retracts to draw the two fluorescent proteins mutually close, increasing FRET efficiency. The dissociation constants for ATP were 7.4 μM to 3.3 mM. ATeams reportedly had ATP levels in the mitochondrial matrix of HeLa cells were significantly lower than those in cytoplasm or in the nucleus. The ATeam was modified to minimize spectral overlap with fluorescence emission of a representative Ca^{2+} indicator fura-2.[74] As the FRET pair, GFP and an orange fluorescent protein (OFP) were used, resulting a substantial red-shift compared to the original ATeam. This improvement enabled simultaneous imaging of both Ca^{2+} and ATP in living cells.

An ATP indicator prepared by organic synthesis was also reported.[75] The ATP indicator has coumarin fluorophore as the FRET donors and a binuclear zinc complex as the FRET acceptor. The zinc complex displayed a large off-on type fluorescence enhancement (33-fold) upon binding to ATP with strong affinity under a neutral aqueous condition. In the nonbonding state, the indicator showed predominantly blue fluorescence from the coumarin unit. The binding of a nucleoside polyphosphate such as ATP induced recovery of the fluorescence of the zinc complex, inducing the marked enhancement of the FRET efficiency. This ATP indicator is applicable to monitor a stimulus-responsive concentration change of ATP.

Temperature Indicators. Temperature influences various biological reactions in living cells. However, the precise mechanism of how the temperature in a tiny intracellular space is controlled and what kind of molecules sense the physical property remains largely unknown. Intensive studies have been dedicated to visualization of intracellular temperature distribution through development of fluorescent thermometers. Uchiyama et al. created a fluorescent nanogel thermometer by combining a thermo-responsive polymer with a water-sensitive fluorophore.[76] This thermometer functioned in living cells and showed high sensitivity to changes in temperature. A weak point in this thermometer is low hydrophilicity, causing aggregation at temperatures higher than 27 °C. To overcome this issue, the fluorescent polymeric thermometer was modified by inducing a hydrophilic unit between the thermo-responsive polymer and water sensitive fluorophore.[77] Using this modified thermometer, the first intracellular mapping based on fluorescence lifetime imaging microscopy (FLIM) was demonstrated. The special resolution of the thermal distribution was at the diffraction-limited level (200 nm) and thermal precision was 0.18−0.58 °C. Using this modified thermometer in combination with fluorescence lifetime imaging microscopy (FLIM), an intracellular map of temperature was created. It revealed the existence of a temperature gradient inside a living cell, suggesting that fundamental cellular processes such as the cell cycle generate an inhomogeneous temperature distribution.

This nanogel thermometer requires the FLIM technique, for which a FLIM setup of apparatus and long time scanning are necessary. In contrast, ratiometric probes allow for quantitative measurement through conventional multicolor fluorescence microscopy. Chiu's group reported nanoparticles working as ratiometric fluorescent thermometers.[78] Temperature sensitive Rhodamine B (RhB) dye was loaded within the matrix of semiconducting polymer dots (Pdots). This Pdot-RhB nanoparticle showed excellent temperature sensitivity and high brightness because of its efficient light harvesting and amplified energy transfer capability of Pdots. Moreover, the Pdot-RhB nanoparticle showed ratiometric temperature sensing under single-wavelength excitation. It has a linear temperature sensing range that matches the physiologically relevant temperatures well.

Another unique fluorescent nanoparticle was developed as a thermometer.[79] This nanoparticle includes europium thenoyltrifluoroacetonate (Eu-TTA) as a temperature sensitive dye, which is embedded in a PMMA network. This particle is further coated with a cationic polymer poly(allylamine hydrochloride) (PAH), which facilitates binding to the anionic plasma membrane. This nanothermometer enters living cells spontaneously via endocytosis, then it is transported along microtubules. The nanothermometer was used to measure the thermal activation of ATPase of motor proteins in living cells by tracking the dynamics and fluorescence intensity of the nanothermometer. The cell temperature increased directly by irradiation of an infrared laser beam for 1 s. The average temperatures before and after heating were, respectively, 36 and 47 °C. The average velocities were, respectively, 0.32, 0.93, and 0.32 μm s^{-1} before, during, and after heating. This method to measure microscopic temperature and molecular activities simultaneously in living cells can shed light on unrevealed cellular processes such as the active transport of organelles.

pH Sensors. Intracellular pH plays crucial roles in cellular function. Regulation of pH is necessary for most cellular process. Many pH sensor molecules used for live imaging are designed to use the FRET technique, but the mechanism differs from that of the above-described FRET sensors such as Ca^{2+} and ATP. Many FRET-based pH sensors do not undergo conformational changes by pH alteration but use differences of pK_a values between the FRET donor and acceptor. Schulz's group developed a novel pH sensor, pHusion, which consisted of a tandem concatenation of EGFP with mRFP1.[80] pHusion worked as a ratiometric pH sensor. Fluorescence of EGFP, of which pK_a is 6.15, is quenched gradually at lower pH values and completely at pH 5, whereas mRFP1, with pK_a of 4.5, is almost entirely insensitive to pH changes in the physiologically relevant ranges. This property allowed for ratiometric measurement of pH changes, where mRFP1 worked as an intramolecular reference.

In addition, the use of FRET between quantum dot and fluorescent protein has been reported.[81] This sensor comprises a pH-insensitive carboxyl-functionalized Q-dot conjugated with pH-sensitive fluorescent proteins mOrange or its homologue, mOrange M163K. Fluorescence microscopy measurements in live cells were performed to demonstrate the ability of the probe to image intracellular pH changes. The probe contained a C-terminal polyarginine sequence, which facilitate endosomal uptake of the probe. This probe visualized the acidification of endosomes in living cells following polyarginine-mediated uptake. These probes have the potential to visualize widely various intracellular pH.

Another design is the use of pH-dependent stability differences between two fluorescent molecules. An EGFP T203Y mutant tethered to a DsRed by a flexible 20 amino acid linker functions as a non-FRET based pH and Cl^- sensor, named ClopHensor.[82] Using this probe, pH and Cl^- concentrations were determined synchronously by comparing fluorescence intensities obtained from different excitations with 458, 488, and 543 nm. Visualization of Cl^- and H^+ fluxes such as large dense-core exocytosis was realized. ClopHensor can be expected to become

dx.doi.org/10.1021/ac3031724 | *Anal. Chem.* 2013, 85, 590−609

a powerful tool for the monitoring of biological processes where Cl^- and H^+ work in a concerted manner.

pH sensors that consist of only a single fluorescent molecule seem more attractive. A mutant of mKeima, a red fluorescent protein with long Stokes shift named pHRed was reported as a single fluorescent molecule pH sensor.[83] Acidification from pH 9 to 6 caused a 7-fold increase in fluorescence intensity at 585 nm, and a 4-fold decrease in the 440 nm fluorescence peak. Both peaks respond with pK_a of 7.8. pHRed is the first ratiometric, single-protein red fluorescent sensor of pH. A variant of mKate that shows a fluorescence color shift depending on the acidic condition will also be available for use for pH sensing.[84] The variants, GmKate, mKate S143C, S158A mutant, are subject to pH-dependent green-to-red color conversion. Crystal structures revealed that potential hydrogen bond networks around the chromophore might facilitate the protonation switch, which induces the bathochromic shift at high pH. GmKate might work as a prototype of genetically encoded monomeric pH sensors for biological studies.

BIOLUMINESCENCE IMAGING AND QUANTITATIVE ANALYSIS

The distinctive benefits of bioluminescence imaging and analysis include the low background, high signal-to-noise (S/N) ratio, wider dynamic range of signals, versatility in the molecular design, and suitability in the imaging of small model animals. Recent studies of bioluminescence imaging are categorized into three divisions: (1) development of new luciferases and synthesis of novel luciferins; (2) protein engineering to create genetically encoded probes with luciferases; and (3) practical application of imaging with the probes such as investigation of cellular function and disease progression. These three are closely mutually correlated in the technical progression. Luciferases with excellent optical properties enable us to design new optical probes with a novel strategy. The new bioluminescent probes are expected to facilitate better optical imaging of molecular phenomenon of interest in living subjects. This section summarizes recent achievements of bioluminescence imaging studies in each division.

Luciferases and Substrates. Luciferases are a family of photoproteins that are isolated from a large variety of insects, marine organisms, and prokaryotes. A wide variety of organisms regulate their light production using different luciferases in various light-emitting reactions. The emission spectra were 400−620 nm. Beetle luciferases, including firefly luciferase (FLuc) and click beetle luciferase (CBLuc), mediate oxidation of D-luciferin in the presence of ATP, Mg^{2+}, and molecular oxygen (O_2).[85] The color emission mechanism was investigated using FLuc variants.[86] However, many marine luciferases from deep-sea organisms catalyze oxidation of coelenterazine only in the presence of O_2. In contrast to beetle and marine luciferases, bacterial luciferases are characteristic in the point that they do not require exogenous substrate supplies for light emissions.[87]

Novel Luciferases. To date, many researchers have devoted their efforts to establishing novel luciferases from new bioluminescent organisms. An engineered luciferase derived from a deep sea shrimp *Oplophorus gracilirostris*, named NLuc, was established by Hall et al.[88] This luciferase molecule is as small as *Gaussia princeps* luciferase (GLuc; 20 kDa) and emits approximately 100-times brighter and more stable bioluminescence than that of *Renilla reniformis* luciferase (RLuc) or FLuc in the presence of coelenterazine (CTZ).

Takenaka et al. discovered *Metridia pacifica* luciferases 1 and 2 (MpLuc1 and 2), which belong to the Metridinidae family, just as *Gaussia princeps* does.[89] In their consecutive research, they also found eleven-copepoda luciferases isolated from the superfamily Augaptiloidea.[90] Although the optical intensities of these copepoda luciferases were not as high as those of GLuc, the identification of new plankton luciferases enriches our knowledge related to luminous organisms in the deep sea and possibly provide new insight into some analytical applications.

Not only establishment of new luciferases but also engineering of conventional luciferases has been conducted frequently to improve the optical properties. Elaborate efforts have been directed to create new variants that exert a brighter, stable, red-shifted bioluminescence. A simple truncation of copepod *Metridia longa* luciferase (MLuc) generated a brighter variant that substantially retains other properties aside from the enhanced optical intensity.[91]

Lehmann et al. previously suggested an *in silico* strategy, the "consensus sequence-driven mutagenesis strategy," to access clues for luciferase engineering.[92] This strategy was chosen on the premise that more frequently occurring amino acids at a given position of the alignment have a stronger thermodynamically stabilizing effect than less frequently occurring amino acids. This strategy was used in modification of RLuc, some variants of which exhibited excellent optical intensity and stability as well as a red-shifted spectral property.[93,94]

Kim et al. also suggested an *in silico* strategy for luciferase engineering, which might be called "alignment and hydrophilicity search".[95,96] Their clues related to luciferase engineering start from high chemical structural similarity between the chromophore of GFP and the common substrate of marine luciferases. It was speculated that GFP variants embed the chromophore inside the molecular backbone, whereas marine luciferases recruit the exogenous luciferin as the chromophore. Marine luciferases are expected to need a hydrophilic interface for efficiently recruiting exogenous luciferin, suggesting a hydrophilicity search to take an initial clue for assuming the interface region of marine or beetle luciferases, e.g., using the scale of Kyte and Doolittle provided by the ExPASy Proteomics Service (Swiss Institute of Bioinformatics; SIB)

Many native luciferases have been improved in terms of their optical properties including a brighter, red-shifted bioluminescence using codon optimization. Codon optimization of native luciferase is a frequently conducted strategy to improve better translational efficiency of the luciferases, by exchanging codons, which are rarely found in the host organism with more frequently observed codons. Motif engineering, such as removal of restriction enzyme recognition sites or addition of immunostimulatory elements, is also often necessary.[97] Now, it appears that codon optimization of luciferases is a fundamental prerequisite for improving the bioluminescence signal in mammalian cells. A new red-emitting codon-optimized mutant of FLuc was developed and used in combination with a green CBLuc, CBG99.[98,99]

An enhanced red-emitting railroad worm luciferase (RWLuc) was also developed through a codon optimization step for bioassays.[100] Nakajima et al. demonstrated a codon-optimized variant of Brazilian click beetle luciferases, named an enhanced green-emitting luciferase (ELuc), which exhibited a 260-fold enhanced optical intensity and red-shifted feature, compared with the wild-type form.[101] Red-shifted variants of CBLuc were used in *in vivo* bioluminescence imaging of two xenograft mouse models for cancer: human hepatoblastoma cell line

dx.doi.org/10.1021/ac3031724 | *Anal. Chem.* 2013, 85, 590−609

(HepG2) and human acute monocytic leukemia cell line (Thp1) cells.[102]

Bacterial luciferases require no infusion or administration of the bioluminescence substrate. However, they are poorly expressed in mammalian cells. To address this limitation, a bacterial luciferase gene cassette (lux) was also codon-optimized for expression in mammalian cell lines.[103]

Substrates for Luciferases. Whereas many luciferases have been extracted from diverse lighting organisms, the luciferins are shared commonly even in different organisms. Commercially available luciferins at the present stage are of only three types: D-luciferin, coelenterazine, and *Cypridina* luciferin. In addition, dinoflagellate and *Latia* luciferins have been identified,[104] although they are used only for biochemical purposes. As the variety of new luciferases has been established, chemical synthesis of new luciferins can be expected to facilitate a better imaging strategy and to foster improvement of the optical properties in the luminous reactions. Chemical synthesis of new luciferins is a fundamental approach to accessing optical properties considering luciferases make use of luciferins as chromophores (luminophores), which is a key for the luminous reaction.

One approach was reported to create a new luciferin precursor, proluciferin acetals, which are oxidized by cytochrome P450 and which produce a D-luciferin for FLuc.[105] Similarly, a D-luciferin precursor was developed for investigating sulfatase activity[106] and caspase-1[107] in the presence of FLuc. This luciferin precursor is also called "caged luciferin".[21] A caged luciferin that releases firefly luciferin was developed for the real-time detection of H_2O_2 within living animals.[108] A phosphine–luciferin conjugate was synthesized for the sensitive detection of azidosugars on a cell surface.[109]

A DEVD peptide-linked D-luciferin, named Z-DEVD-aminoluciferin, was reported for measuring real-time caspase-3/7 activation. In the presence of apoptosis signaling, the Z-DEVD-aminoluciferin is cleaved by caspase 3/7, resulting in the release of aminoluciferin that is free to react with luciferase, generating measurable light.[110] Other luciferins bearing an amino group on a substrate backbone were newly synthesized, where they emit bioluminescence in various colors from green to red.[111] This study was extended further to synthesize a membrane-impermeable bioluminogenic substrate of luciferases.[112]

Theoretical investigations of luminous reactions were also conducted, which included (i) luminous reactions of cypridina luciferin analogues, (ii) a luciferin complexation with heavy metal ions, and (iii) a solvent effect in biological media and interactions between solvents and luciferin.[113−115]

In contrast to fluorescence, the use of a substrate in bioluminescence is an important disadvantage, especially when being used in live cells. The disadvantage originate from the issues of (i) membrane permeability of the substrates and (ii) biased diffusion of the substrate into the compartments of mammalian cells.[116] Furthermore, Hu et al. reported that D-luciferin itself participates in an intracellular signal transduction, e.g., acting as a partial agonist for G protein-coupled receptor-35 (GPCR35).[117]

To address the substrate-driven problems, plasma membrane (PM)-anchoring imaging probes were created for sensing internal signals or extracellular display of the probe.[116,118] Xia et al. also developed a bioluminescent activatable reporter immobilized in the PM.[119] Such localization of the probes on the plasma membrane is a clever strategy from the perspective that alleviates concern about the substrate and O_2 supply.

A water-soluble coelenterazine (s-CTZ) was developed by Morse et al. to address the substrate-driven matters described above.[120] In contrast to native CTZ, s-CTZ exhibited 100-fold greater sensitivity than CTZ *in vitro*, although the chemical structure is the same as native CTZ. They also exhibited that s-CTZ exerts 10-fold higher photon counts than CTZ *in vivo*. The substrate was used for imaging apoptosis signaling *in vivo*.[121]

Coelenterazine-*v* (CTZ-*v*) exerts a remarkably red-shifted spectrum from blue to yellow green with RLuc8.[93] This feature was used for BRET imaging within deep tissues of living mice.[122] However, CTZ-*v* is extremely unstable in solution. The instability was greatly relieved by the linkage of CTZ-*v* with Ca^{2+}-triggered coelenterazine-binding protein (CBP).[123]

Selection of an appropriate luciferase–substrate pair is another important feature. A striking difference in the optical intensities was reported according to the combination. The best combinations recommended were RLuc plus Viviren and GLuc plus native CTZ.[124]

Bioluminescent Probes. Conventional imaging technologies rely mostly on nonspecific, macroscopic, physical, physiological, or metabolic changes that differentiate pathological from normal tissue rather than identifying specific molecular events.[125] Luciferases catalyzing oxidation of luciferins for bioluminescence are a nearly ideal reporter for bioanalysis and molecular imaging of specific intracellular molecular events. Many luciferases were smartly engineered to create novel optical indicators according to the basic concept presented in Figure 2.

Probes for Protein–Protein Interactions. In response to outer signals, proteins in cells take specific actions including the following: (i) protein–protein interactions, (ii) conformation changes, (iii) translocation, and/or (iv) phosphorylation. Many transcription factors activated by ligands change its conformation for protein–protein interaction, and are translocated into the nucleus. Phosphorylation is also necessary for the function of transcription factors in normal cell behavior and tumor growth. Many imaging strategies to access these specific actions of proteins have been developed to date.

Many cases of protein–protein interactions were imaged with a strategy of reconstitution of luciferase fragments, which includes protein fragment complementation assays[126] and intein-mediated protein reconstitution assays.[127] A luciferase is fragmented into two parts, each of which is linked with a protein pair of interest. Upon occurrence of the protein–protein interactions, the adjacent fragments of the luciferase are complemented or reconstituted.

Marine and beetle luciferases were dissected into two fragments to fabricate the probes described above, which are also categorized into two groups: single-chain and two-chain types. History of the protein-complementation strategy started from a study by Richards, who made use of subtilisin-cleaved bovine pancreatic ribonuclease.[128] The advantages of this complementation strategy were well-highlighted in the study reported by Michnick et al., in which they mapped numerous protein–protein interactions in yeast using luciferase fragments.[129,130] They also presented detailed protocols for large-scale analysis of protein–protein interactions with the survival selection based on the protein complementation of dihydrofolate reductase (DHFR) reporter.[126] The basic concept of luciferase complementation was applied to various protein–protein binding models. Ozawa et al. first demonstrated the application

dx.doi.org/10.1021/ac3031724 | *Anal. Chem.* 2013, 85, 590−609

of luciferase reconstitution[127] and extended that study into optimization of split-FLuc probe that detects interaction of the kinase-inducible domain (KID) of cyclic adenosine monophosphate response element binding protein (CREB) and the KIX domain of CBP/p300.[131]

The strategy of complementation of luciferase-fragments was also used for the determination of various protein phosphorylation and caspase activities.[132] This imaging platform facilitates medicinal and pharmaceutical studies including those of oncology and new drug discovery.[133] An epidermal growth factor (EGF) receptor-mediated phosphorylation of the trans-kinase (ErbB2) was visualized using the complementation strategy.[134] Tumor growth factor-β (TGFβ)-activated Smad2/3 phosphorylation was imaged using a split-FLuc.[135] Glycogen synthase kinase-3 (GSK3) is a critical mediator in glycogen metabolism and insulin signaling. Casein kinase-1 (CK1) also acts as critical roles in circadian rhythm, nuclear import, and apoptosis. A molecular imaging tool was developed for real-time illuminating kinase activities of GSK3β and CK1β based on FLuc complementation.[136] A phosphorylation-mediated interaction between glycogen synthase kinase 3β (GSK3 β) and *c*-Myc was visualized using a split-FLuc complementation strategy.[137]

The basic concept was also used for imaging molecular events on the plasma membrane. For instance, interaction of G-protein coupled receptors (GPCRs) with β-arrestin on the plasma membrane was imaged with a set of bioluminescent probes (Figure 5A).[138,139] Similarly, dimerization of extracellular signal-regulated kinase 2 (ERK2) was visualized with a pair of ERK2-linked split-RLuc.[140] The basic concept of protein reconstitution was further extended to multicolor determination of conditional protein−protein interactions according to kinds of the signal, e.g., whether agonistic or antagonistic signals.[141]

A dual-color imaging tool named "luciferase heteroprotein fragment complementation systems" was developed to quantify two discrete pairs of interacting proteins simultaneously or two distinct proteins interacting with a third shared protein in live cells (Figure 5B).[142−144] A Notch signaling pathway was also identified with heteroprotein fragment complementation of two luciferases.[145]

Probes for Small Molecules. Because all known luciferases, without exception, consume molecular oxygen, the role of luciferases was speculated as detoxification of reactive oxygen species (ROS) in cells.[146] This feature implies that luciferase reactions might be useful as an ROS sensor. Furthermore, beetle luciferases such as FLuc and CBLuc catalyze oxidation of luciferins for bioluminescence in the presence of ATP and Mg^{2+}. This luminous reaction can be converted to construction of probes sensing ATP- or Mg^{2+}. In practice, this ATP-sensitive feature of FLuc was used to monitor pathological alterations in β-cell function in the nonobese-diabetic (NOD) mouse model of T1D.[147] Furthermore, an *in vivo* imaging probe with FLuc was also demonstrated to determine H_2O_2 in tumor models for a long period of time using luciferase-expressing mice.[148]

Quantitative imaging of cyclic 3′,5′-monophosphate AMP (cAMP) was conducted with the conditional complementation of split fragments of green and red luciferases originated from click beetles.[144] A homodimerization and heterodimerization of estrogen receptor α and β (ER α and ER β) were visualized using split-FLuc and split-RLuc.[149]

Kim et al. developed a series of probes for which all components including fragments of a luciferase, a ligand-recognition protein (LRP), and linkers are integrated in a single-chain backbone.[150−152] In the presence of a ligand such as estrogen or androgen, the LRP changes its conformation and further induces an internal protein−protein interaction. This intramolecular interaction provokes reconstitution of the fragmented luciferase resurrecting the luciferase activity.

To visualize Ca^{2+} in living cells, Hoshino et al.[153] developed a brighter bioluminescent probe. The "BRET-based autoilluminated fluorescent protein on EYFP (BAF-Y)" probe exhibited extraordinary efficiency in the resonance energy transfer (RET) between a variant of RLuc (RLuc8) and EYFP. The BRET

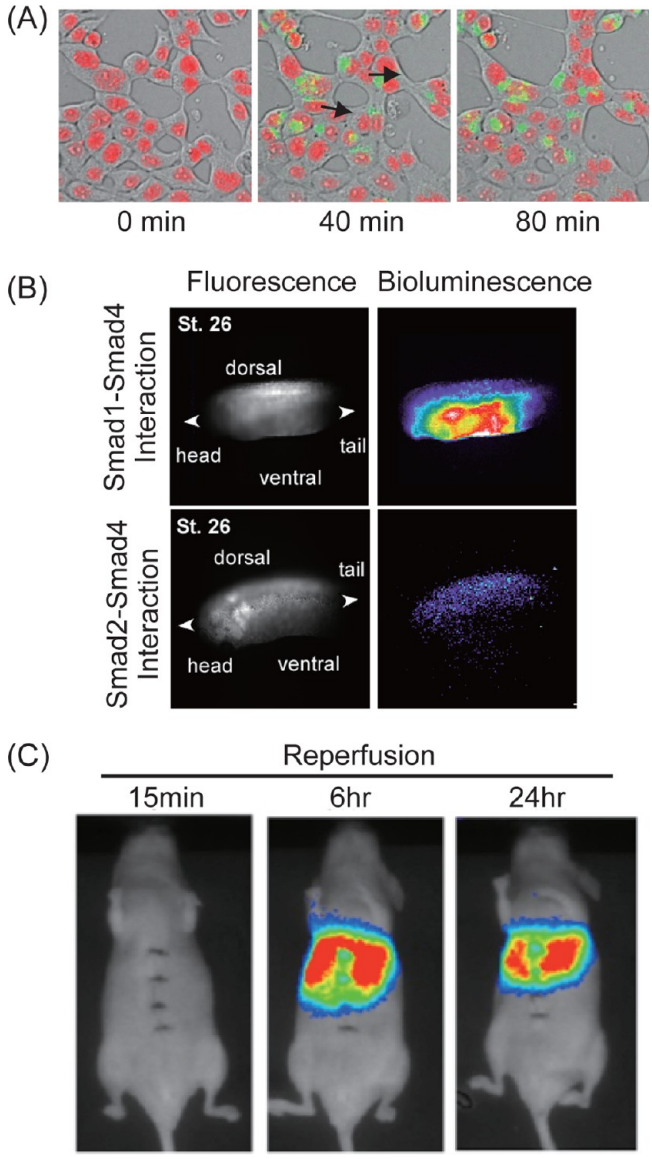

Figure 5. Bioluminescence images of living cells and animals. (A) Bioluminescence images of GPCR-β−arrestin interactions (green). The nuclei label a fluorescent dye, DRAQ5. The fluorescence and bioluminescence images are superimposed on the bright field images. (B) Bioluminescence images of Smad1-Smad4 and Smad1−Smad4 interactions in developing stages of *Xenopus laevis* embryo (right). Fluorescence images of Venus are shown on the right side for identifying the morphology of the embryo. (C) Visualization of caspase-3 activity in living mice. The caspase-3 activation is induced by 1 h of ischemia. The time indicates reperfusion after the ischemia. The bioluminescence intensity is shown with pseudo colors. Reprinted from ref 138. Copyright 2010 American Chemical Society. Reprinted with permission from ref 143. Copyright 2009 Hida et al.

dx.doi.org/10.1021/ac3031724 | *Anal. Chem.* 2013, 85, 590−609

system was also developed for imaging intramolecular interactions between CaM (Ca^{2+}-binding protein) and its binding peptide, M13, which were sandwiched between a yellow fluorescent protein variant, Venus, and an enhanced *Renilla* luciferase, RLuc8.[154]

Probes for Enzymatic Activity. An innovative probe design called "luciferase cyclization" among reporter-reconstitution technologies was reported previously.[8] In the probe design, the N-terminal and C-terminal fragments of FLuc were cyclized via a substrate peptide of caspase-3 (DEVD) (closed circular form). Active caspase-3 digests the DEVD sequence in the circular fusion and linearizes the formation (opened linear form), thereby restoring the FLuc activity. This strategy was used extensively to examine dynamic changes of apoptosis (caspase-3 activity) of a mouse liver, proving that the emitted signals reflected the biochemically evaluated apoptotic cell death (Figure 5C).[155,156]

A BRET probe was developed, where RLuc was linked with QD via a DEVD peptide for sensing caspase-3 activity.[157] A benefit of these BRET-QD probes is self-illumination in near-infrared in the presence of the substrate, with no external radiation.[158] It is particularly interesting that a BRET between bioluminescent bacteria and a fluorophore,[159] between GFP and obelin,[160] and between monomeric red fluorescent protein (mRFP) and aequorin[161] were reported for molecular imaging. In a mouse modality, a lymphatic basin was visualized clearly in BRET imaging with minimal background signals.[162]

Probes for Nucleic Acids. Similarly, an adjacent binding of probes labeled with RLuc and quantum dot (QD) on the nucleic acid target (BRET) was conducted to analyze nucleic acids, where RLuc, a bioluminescent protein that generates light by a chemical reaction, is used as an energy donor, and where QD is used as an energy acceptor.[163] Another heterogeneous imaging probe for nucleic acid detection was realized using a polyconjugate of RLuc8, which was connected directly with a nucleotide and a DABCYL quencher.[164] In the presence of a target nucleotide, RLuc8 releases from the quencher, starting the emission of bioluminescence.

Probes for Gene Expression. A bioassay accompanying luciferase expression, which is called "reporter-gene assay", is prevailing for estimating transcriptional activities of ligands, which include drug candidates, toxic chemicals, endocrine disrupting chemicals (EDC), and hormones, e.g., this assay has been used for screening of anticancer drugs targeting the protein tyrosine phosphatase Shp2.[165] Circadian fluctuations according to the activity of clock gene promoters were imaged in multiple colors using multiple luciferases.[104] Application of the reporter to living subjects is summarized in the following section of Imaging of Living Subjects.

Genomic and nongenomic signaling pathways of steroid hormone receptors have been targeted for molecular imaging. Kim et al. simultaneously imaged the genomic and nongenomic activation of ERα in response to steroids and chemicals using conditional complementation of split-click beetle luciferases green and red (CBLuc green and red).[141] The genomic and nongenomic actions of ER were estimated further using a reporter-gene assay expressing luciferase.[166]

Imaging of Living Subjects. Although QDs possess higher photostability and brightness for imaging living subjects,[162,167] the materials suffer from toxicity and poor *in vivo* biodistribution.[168] The uses of QDs also have limited versatility in the probe design and are deeply restricted by the surface labeling chemistry. We specifically examine bioluminescence imaging (BLI) and luciferase-based molecular probes, where advanced optical properties of light-emitting proteins and smartly designed imaging probes strongly support molecular imaging of living subjects. In conjunction with various noninvasive imaging modalities, cell-labeling methods such as exogenous labeling or transfection with a reporter gene allow visualization of labeled cells *in vivo* in real time, as well as monitoring and quantification of cell accumulation and function, which enables us to ascertain the location, distribution, and long-term viability of the therapeutic cell populations.[169] These imaging strategies using genetic engineering are complex. However, they have the potential to allow highly specific and detailed analyses of living subjects.[170]

Bioluminescence is an excellent optical readout and suitable for biomedical research purposes caused by the extremely low background intensity, high signal-to-noise (S/N) ratio, non-invasive character, short acquisition time (seconds to minutes), and the possibility of measuring many animals simultaneously (high throughput).[171]

The novel luciferases and probes described above have great potential for identifying specific molecular events in living subjects. The three major directions are described below.

Imaging of Disease Progression. Bioluminescence imaging (BLI) is a powerful technology for viral pathogenesis, immune responses to infection, and evaluation of therapy in living subjects. This technique allows longitudinal studies of viral replication and dissemination in the same cohort of mice.[172] To date, many cell- and transgenic mouse-based models have been developed to evaluate viral infection and inflammation in living subjects.

A transgenic reporter mouse with FLuc that is regulated by a herpes simplex virus (HSV)-1 thymidine kinase (TK) promoter was generated for imaging the infection with HSV-1.[173] Another transgenic reporter mouse for BLI of Gal4/upstream activation sequence (UAS) system was developed for imaging adenoviral infection in living subjects.[174] Furthermore, a bidirectional two-step transcriptional amplification (TSTA) system that exerts enhanced transcriptional strength of cancer-specific Survivin promoter was developed to evaluate the intratumoral delivery of adenoviral vector in a hepatocellular carcinoma model.[175]

Viral infection at the cellular level provokes inflammatory responses that recruit immune cells. To visualize transcriptional regulation of immune responses, a luciferase reporter mouse was developed, where the mice revealed dynamics of host immune responses in tissues.[173] Because pro-inflammatory cytokines are expressed by nuclear factor-kappa B (NF-κB), a transgenic reporter mouse for bioluminescence imaging of NF-κB-dependent transcription was generated. This study was further extended with spatial and temporal activation of inflammation by pulmonary endotoxin,[176] ionizing radiation,[177] or by lipopolysaccharide (LPS)[178] and its effects on tissue pathology.

Bacterial migration in living mice was also imaged with bioluminescent bacteria carrying a *luxCDABE* operon.[179] Trafficking of various types of innate and adaptive immune cells to sites of infection is a critical part of the host response to infection.

A transgenic mouse that expresses FLuc in hematopoietic cells was developed for imaging the activation, expansion, and trafficking of T-cells in living mice.[180] A bioluminescence imaging of interferon β expression during viral infection was conducted using a transgenic mouse, in which FLuc was recombined into the genome under control of the endogenous promoter for interferons.[181]

To image neuronal injury *in vivo*, transgenic mice were developed using the promoter for glial fibrillary acid protein

dx.doi.org/10.1021/ac3031724 | *Anal. Chem.* 2013, 85, 590−609

(GFAP) to regulate expression of FLuc.[182] Aggregation of amyloid-β (Aβ) peptides is linked to the pathogenesis of Alzheimer's disease. Aβ deposition was monitored in live mice using bioluminescence imaging (BLI).[183184]

Expression of inducible nitric oxide synthase (iNOS) increases in response to tissue injury, oxidative damage, and high-fat diet to organs and tissues. To examine such tissue injury, oxidative damage,[173] and effects of high-fat diet,[185] a transgenic mouse with FLuc was developed, where expression of FLuc was controlled by the murine iNOS promoter.

As described above, BLI for studying viral infection and inflammation in small animal models of diseases are gaining popularity. This versatile feature of luciferase-aided molecular imaging techniques can be expected to expand the usage of BLI to identify infection and inflammation and to analyze the effects of antiviral and anti-inflammation therapies.

Bacteria present an attractive class of vector for cancer therapy, possessing the natural capability to grow preferentially within tumors following systemic administration. An interesting study was reported for the purpose, where *Salmonella typhimurium* SL7207 expressing the luxABCDE operon were administered intravenously (i.v.) to mice bearing subcutaneous (s.c.) FLuc-expressing xenograft tumors.[186187]

Bacterial luciferases were also used for imaging infection and toxicity. For example, gene expression in bacteria during infections was monitored using an adaptable set of bioluminescent genes (luxCDABE operon).[188189] A flow-through biosensor using agar-immobilized bioluminescent recombinant reporter bacteria was developed for online continuous water toxicity monitoring.[190]

Imaging of Stem Cells and Organs. Major imaging instrumentations for organs might be categorized into five groups: (i) optical bioluminescence and fluorescence imaging techniques, (ii) radionuclide-based positron emission tomography (PET) and single-photon emitted computed tomography (SPECT), (iii) X-ray-based computed tomography (CT), (iv) magnetic resonance imaging (MRI), and (v) ultrasound imaging (US). In addition, bioluminescence is combined further with computed tomography (CT) techniques and named bioluminescence tomography (BLT).[191] The algorithm was studied to ascertain the source locations and strengths accurately and reliably.[192] An example for improving the BLT accuracy was discussed.[193] This BLT allows superearly imaging of tumors *in vivo*.[194] Recent achievements in imaging of embryos and organs can be summarized in greater detail according to different organs.

Brain Imaging. A traditional technique to access the molecular actions in brain is to image neurons from brain slices.[160] In contrast to the *in vitro* approach, current brain imaging is frequently conducted to monitor the temporal kinetics and molecular mechanisms in living transgenic mice. BLI is emerging as a potential means for *in vivo* assessment of intracranial tumor growth and response to therapy in brain, e.g., in rodent orthotopic xenograft models of primary brain malignancies.[195]

Real-time bioluminescence imaging reflecting activity of the transcription factor CCAAT enhancer binding protein (C/EBP) activity was performed in C/EBP-luciferase-expressing mice because C/EBP is involved in inflammatory processes in the nervous system. A striking activity of C/EBP was imaged in the mouse brain, showing that C/EBP mediates the brain response to inflammation.[196]

Lung Imaging. A rat orthotopic lung tumor model was imaged with bioluminescence of FLuc and microcomputed tomography (CT).[197] BLI with FLuc-transfected 4T1 murine breast cancer cells was also conducted to monitor a lung tumor burden noninvasively.[198] The studies described above revealed that bioluminescence intensity correlates directly with the tumor volume.

Imaging Bone Formation. Previously, *in vivo* imaging of bone-forming osteoblasts in musculoskeletal tissue was reported, where the osteoblasts express FLuc under the control of an osteoblast-specific osteocalcin promoter.[199] Hormone actions to osteoblasts and osteoclasts were also imaged with transgenic mice carrying FLuc under control of an estrogen-responsive promoter.

Liver Imaging. Ozaki et al. present an example of *in vivo* imaging of liver states using a luciferase-based caspase-3 optical probe.[155] They examined dynamic changes of apoptosis (caspase-3 activity) of a mouse liver, proving that the emitted signals reflected the biochemically evaluated apoptotic cell death. As the imaging probe, they constructed a cyclic luciferase structure that is initially distorted (inactive form). Once caspase-3 cleaves the DEVD in the cyclic luciferase structure, FLuc changes into an active form, thereby restoring luminescence activity. Interferon β activity and parasite development in liver were determined, respectively, using interferon β promoter-directed FLuc[200] and a transgenic parasite expressing FLuc.[201]

Imaging Embryonic Stem Cells. Embryonic stem (ES) cells hold tremendous therapeutic potential in diseases. Therefore, the corresponding imaging techniques with ES cells have been developed.[202] ES cells expressing FLuc were radiolabeled and then transplanted into early second trimester fetal monkey kidneys. Fetal kidneys were imaged *ex vivo*.[203] Localization and survival of ES cells expressing luciferase was also monitored over time as a preclinical disease model of vascular disease.[204] BLI was also used to image renewal capacity of muscle stem cells on rigid and soft substrates of dishes *in vitro*.[205]

Imaging of Cancers and Their Metastasis. Cancer is a disease for which better understanding of cell signaling potentially engenders improved therapies.[206] One powerful tool that is useful to investigate such a complex cell signaling network is a molecular imaging probe with luciferases. Metastasis as the life-threatening aspect of cancer is a systemic disease process. Consequently, investigation of mechanisms of metastasis might offer new therapeutic options.[207]

Molecular imaging probes embedding a luciferase as an optical reporter provide cost-effective strategies for preclinical small-animal studies. The tagged probes provide a direct linkage to cancer-associated molecules and enable researchers to illuminate molecular dynamics in real time *in vivo*.[208] This approach allows a time course for response to treatment to determine the specific dosage for a desired molecular action.

Luminescent melanoma cells were used to investigate tumor growth and tumor localization with *in vivo* BLI.[209] The growth and metastasis of human bladder cancer, i.e., UM-UC-3 cell stably expressing FLuc, was tracked real-time *in vivo* by bioluminescence.[210] GLuc with cell-secreting nature was used for tumor monitoring in mice and for dual-reporter assessment in combination with FLuc.[211]

Wang et al. optically imaged tumor properties in a human neuroblastoma model and made a detailed map of the tumor progression with the luciferase-positive cancer cells.[212] Drug efficacy of proteasome inhibitors in the treatment of multiple myeloma was also reviewed with BLI.[213] *In vivo* evaluation of anticancer reagents has been conducted, e.g., inhibitors of histone deacetylase (HDAC) activity as anticancer agents.[214] For

dx.doi.org/10.1021/ac3031724 | *Anal. Chem.* 2013, 85, 590−609

identifying tumor-specific biomarkers and for evaluating preclinical drugs, a model transgenic mouse has been used.[215] Investigations of personalized cancer medicines are also emerging recently.[216]

PERSPECTIVE

Imaging technologies have made remarkable progress because of the emergence of various probe molecules. In addition, new techniques based on nonlinear optics increasingly accelerate the development of novel fluorescence imaging techniques, although the topics cannot be included in this review. A super-resolution imaging such as PALM and stochastic optical reconstruction microscopy (STORM) is an exciting field, wherein new fluorescent proteins with a specific spectral character are required. Although we specifically examined the current advancement of the probes, the optical system including the sample condition must always be regarded as well as optical probe molecules. Additional progress in the imaging technology will depend on the synergistic achievements in the development of molecules and probes, microscopic systems including lasers and filters, and software for data analysis.

One current trend in imaging is zooming in on the biological structures beyond the diffraction barrier. Intracellular architecture like organelles comprises proteins and lipids, of which the size is less than 100 nm. To visualize such structures, researchers often use electron microscopy. However, the biological samples must be fixed and molecular information is often lost in conventional electron microscopy. Now, super-resolution fluorescence microscopy can achieve scales of less than 50 nm in live cell imaging, with which we can obtain crucial information of functional molecules as well as intricate structures in the near future.

Zooming out of the image also provides intriguing biological information related to dynamic networks of individual cells in small animal models. Light penetration limits the depth of organs that can be analyzed. The use of visible light invariably limits the applicability of imaging. Intriguingly, it has been demonstrated that materials with photoacoustic character are useful for molecular imaging.[217,218] Acoustic waves travel into tissues deeper than optical light can. Therefore, improvement of photoacoustic materials is expected to break new ground for *in vivo* animal imaging.

Design of new probes is a difficult task. Basic concepts and strategies have emerged. Design might be accomplished by learning from natural organisms and phenomena if we could discover additionally a conceptually novel design of imaging tools. To date, great efforts have been devoted to extraction and identification of luminescent proteins from light-emitting organisms, from which convergence of the optical properties was realized. Such material improvement in the properties is connected directly to advances in smartly designed bioluminescent probes. In fact, protein complementation is a representative mechanism that is useful to control enzymatic activities and signaling cascades in living cells. BRET is a naturally occurring event in luminescent organs such as those of a jelly fish. Protein splicing is a part of protein modification that takes place in prokaryotic cells. Similarly, molecular events in nature might inspire researchers to cultivate new fields of imaging analysis.

The ideal fluorescent molecules for use as bioimaging probes are those that are photostable against bleaching and blinking, which are physically small without perturbation of functions of target molecules and which show high selectivity to the target molecules. In these respects, fluorescent molecules discovered or developed to date present both benefits and shortcomings: genetically encoded fluorescent proteins are easily expressed in living cells, but they are usually photolabile compared to organic fluorescent dyes and fluorescent nanoparticles. Organic fluorescent dyes are small, and fluorescent nanoparticles demonstrate photostability. These fluorophores, however, are not standards as labeling materials for bioimaging because of the difficulty in their selective binding to target molecules. Development of highly photostable fluorescent proteins or of a novel principle to tag an artificial fluorophore specifically to a molecule of interest might produce a breakthrough in bioimaging studies.

A prominent tendency in animal imaging is to connect the luciferase images with a pathological interpretation including disease progression, not only a conventional passive molecular imaging such as cancer metastasis using bioluminescent tumor cells. For this purpose, multimodality imaging is now developing. It is a hybrid of bioluminescence imaging with fluorescence imaging, positron emission tomography, X-ray computed tomography, functional MRI, etc. Improvement of the precision in the modality imaging will allow for animal experiments that can more conveniently aid in drug screening and pathological analysis.

We expect that researchers will devote great efforts to creating smart imaging probes, being truly quantitative, highly sensitive, and readily comprehended. All of these efforts will contribute greatly to realization of excellent imaging of the next generation, which will engender deeper understanding of biological systems and will break new ground in different fields of life science.

AUTHOR INFORMATION

Corresponding Author

*E-mail: ozawa@chem.s.u-tokyo.ac.jp. Phone: +81-3-5841-4351. Fax: +81-3-5802-2989.

Notes

The authors declare no competing financial interest.

Biographies

Takeaki Ozawa received his B.S. degree in 1993 and M.S. degree in 1995 from the University of Tokyo, Japan. He completed the doctoral course at the University of Tokyo, Graduate School of Science, and received his Ph.D in 1998. He served as research associate at the University of Tokyo, and started an independent position of associate professor at the Institute for Molecular Science, Japan. He is in current position of professor at Department of Chemistry, Graduate School of Science, the University of Tokyo. His research interest is "to develop novel analytical methods for visualizing and controlling functions of molecules in living subjects".

Hideaki Yoshimura was born in Osaka, Japan. He graduated from Kyoto University (Japan) in 2001 with a Bachelor's degree in Chemistry. He received his Ph.D from the Graduate University for Advanced Studies (Japan) in 2007. From 2007, he worked as a postdoctoral researcher in Kyoto University (Japan). He is currently a project assistant professor at the University of Tokyo (Japan) since 2009. His current research involves fluorescence live-cell imaging of dynamics of RNAs and signaling molecules especially at the single molecule level.

Sung-Bae Kim studied chemistry at the University of Tokyo (Japan), where he received his Ph.D. degrees in 2004. From 2005 to 2009, he worked for 5 years as a postdoctoral researcher in the National Institute of Advanced Industrial Science and Technology (AIST), Tsukuba (Japan). Since 2010, he became a tenure track researcher at AIST, Tsukuba (Japan). His current research activities include the

development of novel artificial luciferases and intelligent molecular imaging probes, and their application to living subjects.

■ ACKNOWLEDGMENTS

This work was supported by the Japan Society for the Promotion of Science (JSPS), New Energy Industrial Technology Development Organization (NEDO), and Japan Science and Technology Agency (JST), Japan.

■ REFERENCES

(1) Erathodiyil, N.; Ying, J. Y. *Acc. Chem. Res.* **2011**, *44*, 925−935.
(2) Newman, R. H.; Fosbrink, M. D.; Zhang, J. *Chem. Rev.* **2011**, *111*, 3614−3666.
(3) Patterson, G.; Davidson, M.; Manley, S.; Lippincott-Schwartz, J. *Annu. Rev. Phys. Chem.* **2010**, *61*, 345−367.
(4) Ibraheem, A.; Campbell, R. E. *Curr. Opin. Chem. Biol.* **2010**, *14*, 30−36.
(5) Saleh, L.; Perler, F. B. *Chem. Rec.* **2006**, *6*, 183−193.
(6) Ozawa, T.; Natori, Y.; Sako, Y.; Kuroiwa, H.; Kuroiwa, T.; Umezawa, Y. *ACS Chem. Biol.* **2007**, *2*, 176−186.
(7) Xu, M. Q.; Evans, T. C., Jr. *Methods* **2001**, *24*, 257−277.
(8) Kanno, A.; Yamanaka, Y.; Hirano, H.; Umezawa, Y.; Ozawa, T. *Angew. Chem., Int. Ed.* **2007**, *46*, 7595−7599.
(9) Grynkiewicz, G.; Poenie, M.; Tsien, R. Y. *J. Biol. Chem.* **1985**, *260*, 3440−3450.
(10) Prasher, D. C.; Eckenrode, V. K.; Ward, W. W.; Prendergast, F. G.; Cormier, M. J. *Gene* **1992**, *111*, 229−233.
(11) Wu, B.; Piatkevich, K. D.; Lionnet, T.; Singer, R. H.; Verkhusha, V. V. *Curr. Opin. Cell Biol.* **2011**, *23*, 310−317.
(12) Campbell, R. E. *Anal. Chem.* **2009**, *81*, 5972−5979.
(13) Shcherbo, D.; Shemiakina, I. I.; Ryabova, A. V.; Luker, K. E.; Schmidt, B. T.; Souslova, E. A.; Gorodnicheva, T. V.; Strukova, L.; Shidlovskiy, K. M.; Britanova, O. V.; Zaraisky, A. G.; Lukyanov, K. A.; Loschenov, V. B.; Luker, G. D.; Chudakov, D. M. *Nat. Methods* **2010**, *7*, 827−829.
(14) Shcherbo, D.; Murphy, C. S.; Ermakova, G. V.; Solovieva, E. A.; Chepurnykh, T. V.; Shcheglov, A. S.; Verkhusha, V. V.; Pletnev, V. Z.; Hazelwood, K. L.; Roche, P. M.; Lukyanov, S.; Zaraisky, A. G.; Davidson, M. W.; Chudakov, D. M. *Biochem. J.* **2009**, *418*, 567−574.
(15) Lin, M. Z.; McKeown, M. R.; Ng, H. L.; Aguilera, T. A.; Shaner, N. C.; Campbell, R. E.; Adams, S. R.; Gross, L. A.; Ma, W.; Alber, T.; Tsien, R. Y. *Chem. Biol.* **2009**, *16*, 1169−1179.
(16) Filonov, G. S.; Piatkevich, K. D.; Ting, L. M.; Zhang, J.; Kim, K.; Verkhusha, V. V. *Nat. Biotechnol.* **2011**, *29*, 757−761.
(17) Lam, A. J.; St-Pierre, F.; Gong, Y.; Marshall, J. D.; Cranfill, P. J.; Baird, M. A.; McKeown, M. R.; Wiedenmann, J.; Davidson, M. W.; Schnitzer, M. J.; Tsien, R. Y.; Lin, M. Z. *Nat. Methods* **2012**, *9*, 1005−1012.
(18) Goedhart, J.; van Weeren, L.; Hink, M. A.; Vischer, N. O.; Jalink, K.; Gadella, T. W., Jr. *Nat. Methods* **2010**, *7*, 137−139.
(19) Subach, O. M.; Cranfill, P. J.; Davidson, M. W.; Verkhusha, V. V. *PLoS One* **2011**, *6*, e28674.
(20) Subach, O. M.; Entenberg, D.; Condeelis, J. S.; Verkhusha, V. V. *J. Am. Chem. Soc.* **2012**, *134*, 14789−14799.
(21) Ran, C. Z.; Zhang, Z. D.; Hooker, J.; Moore, A. *Mol. Imaging Biol.* **2012**, *14*, 156−162.
(22) Subach, F. V.; Zhang, L.; Gadella, T. W.; Gurskaya, N. G.; Lukyanov, K. A.; Verkhusha, V. V. *Chem. Biol.* **2010**, *17*, 745−755.
(23) Grotjohann, T.; Testa, I.; Leutenegger, M.; Bock, H.; Urban, N. T.; Lavoie-Cardinal, F.; Willig, K. I.; Eggeling, C.; Jakobs, S.; Hell, S. W. *Nature* **2011**, *478*, 204−208.
(24) Brakemann, T.; Stiel, A. C.; Weber, G.; Andresen, M.; Testa, I.; Grotjohann, T.; Leutenegger, M.; Plessmann, U.; Urlaub, H.; Eggeling, C.; Wahl, M. C.; Hell, S. W.; Jakobs, S. *Nat. Biotechnol.* **2011**, *29*, 942−947.
(25) Subach, F. V.; Subach, O. M.; Gundorov, I. S.; Morozova, K. S.; Piatkevich, K. D.; Cuervo, A. M.; Verkhusha, V. V. *Nat. Chem. Biol.* **2009**, *5*, 118−126.
(26) Pletnev, S.; Subach, F. V.; Dauter, Z.; Wlodawer, A.; Verkhusha, V. V. *J. Am. Chem. Soc.* **2010**, *132*, 2243−2253.
(27) Khmelinskii, A.; Keller, P. J.; Bartosik, A.; Meurer, M.; Barry, J. D.; Mardin, B. R.; Kaufmann, A.; Trautmann, S.; Wachsmuth, M.; Pereira, G.; Huber, W.; Schiebel, E.; Knop, M. *Nat. Biotechnol.* **2012**, *30*, 708−714.
(28) Alford, S. C.; Abdelfattah, A. S.; Ding, Y.; Campbell, R. E. *Chem. Biol.* **2012**, *19*, 353−360.
(29) Shcherbakova, D. M.; Hink, M. A.; Joosen, L.; Gadella, T. W.; Verkhusha, V. V. *J. Am. Chem. Soc.* **2012**, *134*, 7913−7923.
(30) Maurel, D.; Banala, S.; Laroche, T.; Johnsson, K. *ACS Chem. Biol.* **2010**, *5*, 507−516.
(31) Kobayashi, T.; Komatsu, T.; Kamiya, M.; Campos, C.; Gonzalez-Gaitan, M.; Terai, T.; Hanaoka, K.; Nagano, T.; Urano, Y. *J. Am. Chem. Soc.* **2012**, *134*, 11153−11160.
(32) Komatsu, T.; Johnsson, K.; Okuno, H.; Bito, H.; Inoue, T.; Nagano, T.; Urano, Y. *J. Am. Chem. Soc.* **2011**, *133*, 6745−6751.
(33) Mizukami, S.; Watanabe, S.; Akimoto, Y.; Kikuchi, K. *J. Am. Chem. Soc.* **2012**, *134*, 1623−1629.
(34) Paige, J. S.; Wu, K. Y.; Jaffrey, S. R. *Science* **2011**, *333*, 642−646.
(35) Paige, J. S.; Nguyen-Duc, T.; Song, W.; Jaffrey, S. R. *Science* **2012**, *335*, 1194.
(36) Melancon, M. P.; Zhou, M.; Li, C. *Acc. Chem. Res.* **2011**, *44*, 947−956.
(37) Iyer, G.; Pinaud, F.; Xu, J.; Ebenstein, Y.; Li, J.; Chang, J.; Dahan, M.; Weiss, S. *Bioconjugate Chem.* **2011**, *22*, 1006−1011.
(38) Choi, Y.; Kim, K.; Hong, S.; Kim, H.; Kwon, Y. J.; Song, R. *Bioconjugate Chem.* **2011**, *22*, 1576−1586.
(39) Sharma, J.; Yeh, H. C.; Yoo, H.; Werner, J. H.; Martinez, J. S. *Chem. Commun.* **2010**, *46*, 3280−3282.
(40) Li, J.; Zhong, X.; Cheng, F.; Zhang, J. R.; Jiang, L. P.; Zhu, J. J. *Anal. Chem.* **2012**, *84*, 4140−4146.
(41) Napp, J.; Behnke, T.; Fischer, L.; Wurth, C.; Wottawa, M.; Katschinski, D. M.; Alves, F.; Resch-Genger, U.; Schaferling, M. *Anal. Chem.* **2011**, *83*, 9039−9046.
(42) He, X.; Wang, Y.; Wang, K.; Chen, M.; Chen, S. *Anal. Chem.* **2012**, *84*, 9056−9064.
(43) Gao, J.; Chen, K.; Luong, R.; Bouley, D. M.; Mao, H.; Qiao, T.; Gambhir, S. S.; Cheng, Z. *Nano Lett.* **2012**, *12*, 281−286.
(44) Wang, H. H.; Lin, C. A.; Lee, C. H.; Lin, Y. C.; Tseng, Y. M.; Hsieh, C. L.; Chen, C. H.; Tsai, C. H.; Hsieh, C. T.; Shen, J. L.; Chan, W. H.; Chang, W. H.; Yeh, H. I. *ACS Nano* **2011**, *5*, 4337−4344.
(45) Batish, M.; Raj, A.; Tyagi, S. *Methods Mol. Biol.* **2011**, *714*, 3−13.
(46) Tyagi, S. *Nat. Methods* **2009**, *6*, 331−338.
(47) Kubota, T.; Ikeda, S.; Yanagisawa, H.; Yuki, M.; Okamoto, A. *PLoS One* **2010**, *5*, e13003.
(48) Kummer, S.; Knoll, A.; Socher, E.; Bethge, L.; Herrmann, A.; Seitz, O. *Angew. Chem., Int. Ed.* **2011**, *50*, 1931−1934.
(49) Vargas, D. Y.; Shah, K.; Batish, M.; Levandoski, M.; Sinha, S.; Marras, S. A.; Schedl, P.; Tyagi, S. *Cell* **2011**, *147*, 1054−1065.
(50) Grünwald, D.; Singer, R. H. *Nature* **2010**, *467*, 604−607.
(51) Lionnet, T.; Czaplinski, K.; Darzacq, X.; Shav-Tal, Y.; Wells, A. L.; Chao, J. A.; Park, H. Y.; de Turris, V.; Lopez-Jones, M.; Singer, R. H. *Nat. Methods* **2011**, *8*, 165−170.
(52) Ozawa, T.; Natori, Y.; Sato, M.; Umezawa, Y. *Nat. Methods* **2007**, *4*, 413−419.
(53) Yamada, T.; Yoshimura, H.; Inaguma, A.; Ozawa, T. *Anal. Chem.* **2011**, *83*, 5708−5714.
(54) Yoshimura, H.; Inaguma, A.; Yamada, T.; Ozawa, T. *ACS Chem. Biol.* **2012**, *7*, 999−1005.
(55) Tilsner, J.; Linnik, O.; Christensen, N. M.; Bell, K.; Roberts, I. M.; Lacomme, C.; Oparka, K. J. *Plant J.* **2009**, *57*, 758−770.
(56) Fosbrink, M.; Aye-Han, N. N.; Cheong, R.; Levchenko, A.; Zhang, J. *Proc. Natl. Acad. Sci. U.S.A.* **2010**, *107*, 5459−5464.
(57) Gavet, O.; Pines, J. *Dev. Cell* **2010**, *18*, 533−543.
(58) Komatsu, N.; Aoki, K.; Yamada, M.; Yukinaga, H.; Fujita, Y.; Kamioka, Y.; Matsuda, M. *Mol. Biol. Cell* **2011**, *22*, 4647−4656.

(59) Gulyani, A.; Vitriol, E.; Allen, R.; Wu, J.; Gremyachinskiy, D.; Lewis, S.; Dewar, B.; Graves, L. M.; Kay, B. K.; Kuhlman, B.; Elston, T.; Hahn, K. M. *Nat. Chem. Biol.* **2011**, *7*, 437−444.
(60) Nakai, J.; Ohkura, M.; Imoto, K. *Nat. Biotechnol.* **2001**, *19*, 137−141.
(61) Tallini, Y. N.; Ohkura, M.; Choi, B. R.; Ji, G.; Imoto, K.; Doran, R.; Lee, J.; Plan, P.; Wilson, J.; Xin, H. B.; Sanbe, A.; Gulick, J.; Mathai, J.; Robbins, J.; Salama, G.; Nakai, J.; Kotlikoff, M. I. *Proc. Natl. Acad. Sci. U.S.A.* **2006**, *103*, 4753−4758.
(62) Dreosti, E.; Odermatt, B.; Dorostkar, M. M.; Lagnado, L. *Nat. Methods* **2009**, *6*, 883−889.
(63) Shigetomi, E.; Kracun, S.; Sofroniew, M. V.; Khakh, B. S. *Nat. Neurosci.* **2010**, *13*, 759−766.
(64) Muto, A.; Ohkura, M.; Kotani, T.; Higashijima, S.; Nakai, J.; Kawakami, K. *Proc. Natl. Acad. Sci. U.S.A.* **2011**, *108*, 5425−5430.
(65) Tian, L.; Hires, S. A.; Mao, T.; Huber, D.; Chiappe, M. E.; Chalasani, S. H.; Petreanu, L.; Akerboom, J.; McKinney, S. A.; Schreiter, E. R.; Bargmann, C. I.; Jayaraman, V.; Svoboda, K.; Looger, L. L. *Nat. Methods* **2009**, *6*, 875−881.
(66) Borghuis, B. G.; Tian, L.; Xu, Y.; Nikonov, S. S.; Vardi, N.; Zemelman, B. V.; Looger, L. L. *J. Neurosci.* **2011**, *31*, 2855−2867.
(67) Zhao, Y.; Araki, S.; Wu, J.; Teramoto, T.; Chang, Y. F.; Nakano, M.; Abdelfattah, A. S.; Fujiwara, M.; Ishihara, T.; Nagai, T.; Campbell, R. E. *Science* **2011**, *333*, 1888−1891.
(68) Ohkura, M.; Sasaki, T.; Kobayashi, C.; Ikegaya, Y.; Nakai, J. *PLoS One* **2012**, *7*, e39933.
(69) Miyawaki, A.; Llopis, J.; Heim, R.; McCaffery, J. M.; Adams, J. A.; Ikura, M.; Tsien, R. Y. *Nature* **1997**, *388*, 882−887.
(70) Nagai, T.; Yamada, S.; Tominaga, T.; Ichikawa, M.; Miyawaki, A. *Proc. Natl. Acad. Sci. U.S.A.* **2004**, *101*, 10554−10559.
(71) Horikawa, K.; Yamada, Y.; Matsuda, T.; Kobayashi, K.; Hashimoto, M.; Matsu-ura, T.; Miyawaki, A.; Michikawa, T.; Mikoshiba, K.; Nagai, T. *Nat. Methods* **2010**, *7*, 729−732.
(72) Si, D.; Epstein, T.; Lee, Y. E.; Kopelman, R. *Anal. Chem.* **2012**, *84*, 978−986.
(73) Imamura, H.; Nhat, K. P.; Togawa, H.; Saito, K.; Iino, R.; Kato-Yamada, Y.; Nagai, T.; Noji, H. *Proc. Natl. Acad. Sci. U.S.A.* **2009**, *106*, 15651−15656.
(74) Nakano, M.; Imamura, H.; Nagai, T.; Noji, H. *ACS Chem. Biol.* **2011**, *6*, 709−715.
(75) Kurishita, Y.; Kohira, T.; Ojida, A.; Hamachi, I. *J. Am. Chem. Soc.* **2010**, *132*, 13290−13299.
(76) Gota, C.; Okabe, K.; Funatsu, T.; Harada, Y.; Uchiyama, S. *J. Am. Chem. Soc.* **2009**, *131*, 2766−2767.
(77) Okabe, K.; Inada, N.; Gota, C.; Harada, Y.; Funatsu, T.; Uchiyama, S. *Nat Commun.* **2012**, *3*, 705.
(78) Ye, F.; Wu, C.; Jin, Y.; Chan, Y. H.; Zhang, X.; Chiu, D. T. *J. Am. Chem. Soc.* **2011**, *133*, 8146−8149.
(79) Oyama, K.; Takabayashi, M.; Takei, Y.; Arai, S.; Takeoka, S.; Ishiwata, S.; Suzuki, M. *Lab Chip* **2012**, *12*, 1591−1593.
(80) Gjetting, K. S. K.; Ytting, C. K.; Schulz, A.; Fuglsang, A. T. *J. Exp. Bot.* **2012**, *63*, 3207−3218.
(81) Dennis, A. M.; Rhee, W. J.; Sotto, D.; Dublin, S. N.; Bao, G. *ACS Nano* **2012**, *6*, 2917−2924.
(82) Arosio, D.; Ricci, F.; Marchetti, L.; Gualdani, R.; Albertazzi, L.; Beltram, F. *Nat. Methods* **2010**, *7*, 516−518.
(83) Tantama, M.; Hung, Y. P.; Yellen, G. *J. Am. Chem. Soc.* **2011**, *133*, 10034−10037.
(84) Wang, Q.; Byrnes, L. J.; Shui, B.; Rohrig, U. F.; Singh, A.; Chudakov, D. M.; Lukyanov, S.; Zipfel, W. R.; Kotlikoff, M. I.; Sondermann, H. *PLoS One* **2011**, *6*, e23513.
(85) Kim, S. B.; Tao, H.; Umezawa, Y. *Cellular and Biomolecular Recognition*; Jelinek, R., Ed.; Wiley-VCH: Darmstadt, Germany, 2009; p 299.
(86) Hosseinkhani, S. *Cell. Mol. Life Sci.* **2011**, *68*, 1167−1182.
(87) Gahan, C. G. M. *Curr. Gene Ther.* **2012**, *12*, 12−19.
(88) Hall, M. P.; Unch, J.; Binkowski, B. F.; Valley, M. P.; Butler, B. L.; Wood, M. G.; Otto, P.; Zimmerman, K.; Vidugiris, G.; Machleidt, T.; Robers, M. B.; Benink, H. A.; Eggers, C. T.; Slater, M. R.; Meisenheimer, P. L.; Klaubert, D. H.; Fan, F.; Encell, L. P.; Wood, K. V. *ACS Chem. Biol.* **2012**, *7*, 1848−1857.
(89) Takenaka, Y.; Masuda, H.; Yamaguchi, A.; Nishikawa, S.; Shigeri, Y.; Yoshida, Y.; Mizuno, H. *Gene* **2008**, *425*, 28−35.
(90) Takenaka, Y.; Yamaguchi, A.; Tsuruoka, N.; Torimura, M.; Gojobori, T.; Shigeri, Y. *Mol. Biol. Evol.* **2012**, *29*, 1669−1681.
(91) Markova, S. V.; Burakova, L. P.; Vysotski, E. S. *Biochem. Biophys. Res. Commun.* **2012**, *417*, 98−103.
(92) Lehmann, M.; Loch, C.; Middendorf, A.; Studer, D.; Lassen, S. F.; Pasamontes, L.; van Loon, A. P. G. M.; Wyss, M. *Protein Eng.* **2002**, *15*, 403−411.
(93) Loening, A. M.; Dragulescu-Andrasi, A.; Gambhir, S. S. *Nat. Methods* **2010**, *7*, 5−6.
(94) Loening, A. M.; Wu, A. M.; Gambhir, S. S. *Nat. Methods* **2007**, *4*, 641−643.
(95) Kim, S. B.; Suzuki, H.; Sato, M.; Tao, H. *Anal. Chem.* **2011**, *83*, 8732−8740.
(96) Kim, S. B. *Protein Eng. Des. Sel.* **2012**, *25*, 1−9.
(97) Condon, A.; Thachuk, C. *Comb. Algorithms* **2011**, *7056*, 337−348.
(98) Caysa, H.; Jacob, R.; Muther, N.; Branchini, B.; Messerle, M.; Soling, A. *Photochem. Photobiol. Sci.* **2009**, *8*, 52−56.
(99) Mezzanotte, L.; Que, I.; Kaijzel, E.; Branchini, B.; Roda, A.; Lowik, C. *PLoS One* **2011**, *6*, e19277.
(100) Li, X. Y.; Nakajima, Y.; Niwa, K.; Viviani, V. R.; Ohmiya, Y. *Protein Sci.* **2010**, *19*, 26−33.
(101) Nakajima, Y.; Yamazaki, T.; Nishii, S.; Noguchi, T.; Hoshino, H.; Niwa, K.; Viviani, V. R.; Ohmiya, Y. *PLoS One* **2010**, *5*, e10011.
(102) Mezzanotte, L.; Fazzina, R.; Michelini, E.; Tonelli, R.; Pession, A.; Branchini, B.; Roda, A. *Mol. Imaging Biol.* **2010**, *12*, 406−414.
(103) Close, D. M.; Patterson, S. S.; Ripp, S.; Baek, S. J.; Sanseverino, J.; Sayler, G. S. *PLoS One* **2010**, *5*, e12441.
(104) Nakajima, Y.; Ohmiya, Y. *Expert Opin. Drug Discovery* **2010**, *5*, 835−849.
(105) Meisenheimer, P. L.; Uyeda, H. T.; Ma, D. P.; Sobol, M.; McDougall, M. G.; Corona, C.; Simpson, D.; Klaubert, D. H.; Cali, J. J. *Drug Metab. Dispos.* **2011**, *39*, 2403−2410.
(106) Rush, J. S.; Beatty, K. E.; Bertozzi, C. R. *ChemBioChem* **2010**, *11*, 2096−2099.
(107) Kindermann, M.; Roschitzki-Voser, H.; Caglic, D.; Repnik, U.; Miniejew, C.; Mittl, P. R. E.; Kosec, G.; Grutter, M. G.; Turk, B.; Wendt, K. U. *Chem. Biol.* **2010**, *17*, 999−1007.
(108) Van de Bittner, G. C.; Dubikovskaya, E. A.; Bertozzi, C. R.; Chang, C. J. *Proc. Natl. Acad. Sci. U.S.A.* **2010**, *107*, 21316−21321.
(109) Cohen, A. S.; Dubikovskaya, E. A.; Rush, J. S.; Bertozzi, C. R. *J. Am. Chem. Soc.* **2010**, *132*, 8563−8565.
(110) Scabini, M.; Stellari, F.; Cappella, P.; Rizzitano, S.; Texido, G.; Pesenti, E. *Apoptosis* **2011**, *16*, 198−207.
(111) Takakura, H.; Sasakura, K.; Ueno, T.; Urano, Y.; Terai, T.; Hanaoka, K.; Tsuboi, T.; Nagano, T. *Chem. Asian J.* **2010**, *5*, 2053−2061.
(112) Takakura, H.; Kojima, R.; Urano, Y.; Terai, T.; Hanaoka, K.; Nagano, T. *Chem. Asian J.* **2011**, *6*, 1800−1810.
(113) Sun, Y.; Ren, A. M.; Min, C. G.; Zou, L. Y.; Ren, X. F. *Acta Phys.-Chim. Sin.* **2010**, *26*, 2779−2786.
(114) Sarasia, E. M.; Afsharnezhad, S.; Honarparvar, B.; Mollaamin, F.; Monajjemi, M. *Phys. Chem. Liq.* **2011**, *49*, 561−571.
(115) Riahi, S.; Abdolahzadeh, S.; Faridbod, F.; Chaichi, M. J.; Ganjali, M. R.; Norouzi, P. *J. Mol. Liq.* **2010**, *157*, 51−56.
(116) Kim, S. B.; Ito, Y.; Torimura, M. *Bioconjugate Chem.* **2012**, *23*, 2221−2228.
(117) Hu, H. B.; Deng, H. Y.; Fang, Y. *PLoS One* **2012**, *7*, e34934.
(118) Santos, E. B.; Yeh, R.; Lee, J.; Nikhamin, Y.; Punzalan, B.; Punzalan, B.; La Perle, K.; Larson, S. M.; Sadelain, M.; Brentjens, R. J. *Nat. Med.* **2009**, *15*, 338−344.
(119) Xia, Z. Y.; Xing, Y.; Jeon, J.; Kim, Y. P.; Gall, J.; Dragulescu-Andrasi, A.; Gambhir, S. S.; Rao, J. *ACS Chem. Biol.* **2011**, *6*, 1117−1126.
(120) Morse, D.; Tannous, B. A. *Mol. Ther.* **2012**, *20*, 692−693.
(121) Niers, J. M.; Kerami, M.; Pike, L.; Lewandrowski, G.; Tannous, B. A. *Mol. Ther.* **2011**, *19*, 1090−1096.

(122) Dragulescu-Andrasi, A.; Chan, C. T.; De, A.; Massoud, T. F.; Gambhir, S. S. *Proc. Natl. Acad. Sci. U.S.A.* **2011**, *108*, 12060−12065.
(123) Stepanyuk, G. A.; Unch, J.; Malikova, N. P.; Markova, S. V.; Lee, J.; Vysotski, E. S. *Anal. Bioanal. Chem.* **2010**, *398*, 1809−1817.
(124) Kimura, T.; Hiraoka, K.; Kasahara, N.; Logg, C. R. *J. Gene. Med.* **2010**, *12*, 528−537.
(125) Massoud, T. F.; Gambhir, S. S. *Genes Dev.* **2003**, *17*, 545−580.
(126) Michnick, S. W.; Ear, P. H.; Landry, C.; Malleshaiah, M. K.; Messier, V. *Meth. Enzymol.* **2010**, *470*, 335−368.
(127) Ozawa, T.; Kaihara, A.; Sato, M.; Tachihara, K.; Umezawa, Y. *Anal. Chem.* **2001**, *73*, 2516−2521.
(128) Richards, F. *Proc. Natl. Acad. Sci. U.S.A.* **1958**, *44*, 162−166.
(129) Tarassov, K.; Messier, V.; Landry, C. R.; Radinovic, S.; Molina, M. M.; Shames, I.; Malitskaya, Y.; Vogel, J.; Bussey, H.; Michnick, S. W. *Science* **2008**, *320*, 1465−1470.
(130) Levy, E. D.; Landry, C. R.; Michnick, S. W. *Science* **2010**, *328*, 983−984.
(131) Ishimoto, T.; Mano, H.; Ozawa, T.; Mori, H. *Bioconjugate Chem.* **2012**, *23*, 923−932.
(132) Shekhawat, S. S.; Campbell, S. T.; Ghosh, I. *ChemBioChem* **2011**, *12*, 2353−2364.
(133) Nyati, S.; Ross, B. D.; Rehemtulla, A.; Bhojani, M. S. *Cancer Cell Int.* **2010**, *10*, 23.
(134) Macdonald-Obermann, J. L.; Piwnica-Worms, D.; Pike, L. J. *Proc. Natl. Acad. Sci. U.S.A.* **2012**, *109*, 137−142.
(135) Nyati, S.; Schinske, K.; Ray, D.; Nyati, M.; Ross, B. D.; Rehemtulla, A. *Clin. Cancer Res.* **2011**, *17*, 7424−7439.
(136) Nyati, S.; Ranga, R.; Ross, B. D.; Rehemtulla, A.; Bhojani, M. S. *Anal. Biochem.* **2010**, *405*, 246−254.
(137) Fan-Minogue, H.; Cao, Z. W.; Paulmurugan, R.; Chan, C. T.; Massoud, T. F.; Felsher, D. W.; Gambhir, S. S. *Proc. Natl. Acad. Sci. U.S.A.* **2010**, *107*, 15892−15897.
(138) Misawa, N.; Kafi, A. K. M.; Hattori, M.; Miura, K.; Masuda, K.; Ozawa, T. *Anal. Chem.* **2010**, *82*, 2552−2560.
(139) Takakura, H.; Hattori, M.; Takeuchi, M.; Ozawa, T. *ACS Chem. Biol.* **2012**, *7*, 901−910.
(140) Kaihara, A.; Umezawa, Y. *Chem. Asian J.* **2008**, *3*, 38−45.
(141) Kim, S. B.; Umezawa, Y.; Kanno, K. A.; Tao, H. *ACS Chem. Biol.* **2008**, *3*, 359−372.
(142) Villalobos, V.; Naik, S.; Bruinsma, M.; Dothager, R. S.; Pan, M. H.; Samrakandi, M.; Moss, B.; Elhammali, A.; Piwnica-Worms, D. *Chem. Biol.* **2010**, *17*, 1018−1029.
(143) Hida, N.; Awais, M.; Takeuchi, M.; Ueno, N.; Tashiro, M.; Takagi, C.; Singh, T.; Hayashi, M.; Ohmiya, Y.; Ozawa, T. *PLoS One* **2009**, *4*, e5868.
(144) Takeuchi, M.; Nagaoka, Y.; Yamada, T.; Takakura, H.; Ozawa, T. *Anal. Chem.* **2010**, *82*, 9306−9313.
(145) Ilagan, M. X. G.; Lim, S.; Fulbright, M.; Piwnica-Worms, D.; Kopan, R. *Sci. Signal.* **2011**, *4*, rs7.
(146) McElroy, W. D.; Seliger, H. H.; White, E. H. *Photochem. Photobiol.* **1969**, *10*, 153−170.
(147) Sever, D.; Eldor, R.; Sadoun, G.; Amior, L.; Dubois, D.; Boitard, C.; Aflalo, C.; Melloul, D. *FASEB J.* **2011**, *25*, 676−684.
(148) Schaferling, M.; Grogel, D. B. M.; Schreml, S. *Microchim. Acta* **2011**, *174*, 1−18.
(149) Paulmurugan, R.; Tamrazi, A.; Massoud, T. F.; Katzenellenbogen, J. A.; Gambhir, S. S. *Mol. Endocrinol.* **2011**, *25*, 2029−2040.
(150) Kim, S. B.; Awais, M.; Sato, M.; Umezawa, Y.; Tao, H. *Anal. Chem.* **2007**, *79*, 1874−1880.
(151) Kim, S. B.; Sato, M.; Tao, H. *Anal. Chem.* **2009**, *81*, 3760−3768.
(152) Kim, S. B.; Takenaka, Y.; Torimura, M. *Bioconjugate Chem.* **2011**, *22*, 1835−1841.
(153) Hoshino, H.; Nakajima, Y.; Ohmiya, Y. *Nat. Methods* **2007**, *4*, 637−639.
(154) Saito, K.; Hatsugai, N.; Horikawa, K.; Kobayashi, K.; Matsu-ura, T.; Mikoshiba, K.; Nagai, T. *PLoS One* **2010**, *5*, e9935.
(155) Ozaki, M.; Haga, S.; Ozawa, T. *Theranostics* **2012**, *2*, 207−214.
(156) Haga, S.; Morita, N.; Irani, K.; Fujiyoshi, M.; Ogino, T.; Ozawa, T.; Ozaki, M. *Lab. Invest.* **2010**, *90*, 1718−1726.
(157) Kim, Y. P.; Daniel, W. L.; Xia, Z. Y.; Xie, H. X.; Mirkin, C. A.; Rao, J. H. *Chem. Commun.* **2010**, *46*, 76−78.
(158) Kosaka, N.; McCann, T. E.; Mitsunaga, M.; Choyke, P. L.; Kobayashi, H. *Nanomedicine* **2010**, *5*, 765−776.
(159) Dragavon, J.; Blazquez, S.; Rekiki, A.; Samson, C.; Theodorou, I.; Rogers, K. L.; Tournebize, R.; Shorte, S. L. *Proc. Natl. Acad. Sci. U.S.A.* **2012**, *109*, 8890−8895.
(160) Drobac, E.; Tricoire, L.; Chaffotte, A. F.; Guiot, E.; Lambolez, B. *J. Neurosci. Res.* **2010**, *88*, 695−711.
(161) Bakayan, A.; Vaquero, C. F.; Picazo, F.; Llopis, J. *PLoS One* **2011**, *6*, e19520.
(162) Kosaka, N.; Mitsunaga, M.; Bhattacharyya, S.; Miller, S. C.; Choyke, P. L.; Kobayashi, H. *Contrast Media Mol. Imaging* **2011**, *6*, 55−59.
(163) Kumar, M.; Zhang, D. H.; Broyles, D.; Deo, S. K. *Biosens. Bioelectron.* **2011**, *30*, 133−139.
(164) Hunt, E. A.; Deo, S. K. *Chem. Commun.* **2011**, *47*, 9393−9395.
(165) Chen, L. W.; Pernazza, D.; Scott, L. M.; Lawrence, H. R.; Ren, Y. A.; Luo, Y. T.; Wu, X.; Sung, S. S.; Guida, W. C.; Sebti, S. M.; Lawrence, N. J.; Wu, J. *Biochem. Pharmacol.* **2010**, *80*, 801−810.
(166) Gambino, Y. P.; Maymo, J. L.; Perez-Perez, A.; Duenas, J. L.; Sanchez-Margalet, V.; Calvo, J. C.; Varone, C. L. *Biol. Reprod.* **2010**, *83*, 42−51.
(167) Wagner, M. K.; Li, F.; Li, J. J.; Li, X. F.; Le, X. C. *Anal. Bioanal. Chem.* **2010**, *397*, 3213−3224.
(168) Resch-Genger, U.; Grabolle, M.; Cavaliere-Jaricot, S.; Nitschke, R.; Nann, T. *Nat. Methods* **2008**, *5*, 763−775.
(169) Kircher, M. F.; Gambhir, S. S.; Grimm, J. *Nat. Rev. Clin. Oncol.* **2011**, *8*, 677−688.
(170) Gross, S.; Piwnica-Worms, D. *Cancer Cell* **2005**, *7*, 5−15.
(171) Snoeks, T. J. A.; Lowik, C.; Kaijzel, E. L. *Angiogenesis* **2010**, *13*, 135−147.
(172) Close, D. M.; Xu, T. T.; Sayler, G. S.; Ripp, S. *Sensors* **2011**, *11*, 180−206.
(173) Luker, K. E.; Luker, G. D. *Antiviral Res.* **2010**, *86*, 93−100.
(174) Pichler, A.; Prior, J. L.; Luker, G. D.; Piwnica-Worms, D. *Proc. Natl. Acad. Sci. U.S.A.* **2008**, *105*, 15932−15937.
(175) Kim, Y. I.; Ahn, B. C.; Ronald, J. A.; Katzenberg, R.; Singh, A.; Paulmurugan, R.; Ray, S.; Gambhir, S. S.; Hofmann, L. V. *J. Vasc. Interv. Radiol.* **2012**, *23*, 704−711.
(176) Hadina, S.; Wohlford-Lenane, C. L.; Thorne, P. S. *Toxicology* **2012**, *291*, 133−138.
(177) Chang, C. T.; Lin, H.; Ho, T. Y.; Li, C. C.; Lo, H. Y.; Wu, S. L.; Huang, Y. F.; Liang, J. A.; Hsiang, C. Y. *PLoS One* **2011**, *6*, e23682.
(178) Vykhovanets, E. V.; MacLennan, G. T.; Vykhovanets, O. V.; Cherullo, E. E.; Ponsky, L. E.; Gupta, S. *J. Urol.* **2012**, *187*, 330−337.
(179) Lee, B. I.; Min, J.-J. *Open Nucl. Med. J.* **2010**, *2010*, 157−165.
(180) Na, I. K.; Markley, J. C.; Tsai, J. J.; Yim, N. L.; Beattie, B. J.; Klose, A. D.; Holland, A. M.; Ghosh, A.; Rao, U. K.; Stephan, M. T.; Serganova, I.; Santos, E. B.; Brentjens, R. J.; Blasberg, R. G.; Sadelain, M.; van den Brink, M. R. M. *Blood* **2010**, *116*, E18−E25.
(181) Pulverer, J. E.; Rand, U.; Lienenklaus, S.; Kugel, D.; Zietara, N.; Kochs, G.; Naumann, R.; Weiss, S.; Staeheli, P.; Hauser, H.; Koster, M. *J. Virol.* **2010**, *84*, 8626−8638.
(182) Cho, W.; Hagemann, T. L.; Johnson, D. A.; Johnson, J. A.; Messing, A. *J. Neurochem.* **2009**, *110*, 343−351.
(183) Stohr, J.; Watts, J. C.; Mensinger, Z. L.; Oehler, A.; Grillo, S. K.; DeArmond, S. J.; Prusiner, S. B.; Giles, K. *Proc. Natl. Acad. Sci. U.S.A.* **2012**, *109*, 11025−11030.
(184) Watts, J. C.; Giles, K.; Grillo, S. K.; Lemus, A.; DeArmond, S. J.; Prusiner, S. B. *Proc. Natl. Acad. Sci. U.S.A.* **2011**, *108*, 2528−2533.
(185) Terashima, M.; Ehara, S.; Yang, E.; Kosuge, H.; Tsao, P. S.; Quertermous, T.; Contag, C. H.; McConnell, M. V. *Mol. Imaging Biol.* **2011**, *13*, 1061−1066.
(186) Cronin, M.; Akin, A. R.; Collins, S. A.; Meganck, J.; Kim, J. B.; Baban, C. K.; Joyce, S. A.; van Dam, G. M.; Zhang, N.; van Sinderen, D.;

O'Sullivan, G. C.; Kasahara, N.; Gahan, C. G.; Francis, K. P.; Tangney, M. *PLoS One* **2012**, *7*, e30940.
(187) Cronin, M.; Collins, S.; Baban, C.; Francis, K.; O'Sullivan, G. C.; Tangney, M. *Mol. Ther.* **2012**, *20*, S267−S267.
(188) Uliczka, F.; Pisano, F.; Kochut, A.; Opitz, W.; Herbst, K.; Stolz, T.; Dersch, P. *PLoS One* **2011**, *6*, e20425.
(189) Waidmann, M. S.; Bleichrodt, F. S.; Laslo, T.; Riedel, C. U. *Bioeng. Bugs* **2011**, *2*, 8−16.
(190) Elad, T.; Almog, R.; Yagur-Kroll, S.; Levkov, K.; Melamed, S.; Shacham-Diamand, Y.; Belkin, S. *Environ. Sci. Technol.* **2011**, *45*, 8536−8544.
(191) Wang, G.; Cong, W.; Durairaj, K.; Qian, X.; Shen, H.; Sinn, P.; Hoffman, E.; McLennan, G.; Henry, M. *Opt. Express* **2006**, *14*, 7801−7809.
(192) Cong, A.; Cong, W. X.; Lu, Y. J.; Santago, P.; Chatziioannou, A.; Wang, G. *IEEE Trans. Biomed. Eng.* **2010**, *57*, 2229−2238.
(193) Klose, A. D.; Beattie, B. J.; Dehghani, H.; Vider, L.; Le, C.; Ponomarev, V.; Blasberg, R. *Med. Phys.* **2010**, *37*, 329−338.
(194) Liu, J. T.; Wang, Y. B.; Qu, X. C.; Li, X. S.; Ma, X. P.; Han, R. Q.; Hu, Z. H.; Chen, X. L.; Sun, D. D.; Zhang, R. Q.; Chen, D. F.; Chen, D.; Chen, X. Y.; Liang, J. M.; Cao, F.; Tian, J. *Opt. Express* **2010**, *18*, 13102−13113.
(195) Dinca, E. B.; Voicu, R. V.; Ciurea, A. V. *Neurosurg. Rev.* **2010**, *33*, 385−393.
(196) de Heredia, L. L.; Gengatharan, A.; Foster, J.; Mather, S.; Magoulas, C. *Neurosci. Lett.* **2011**, *497*, 134−138.
(197) Saha, D.; Watkins, L.; Yin, Y.; Thorpe, P.; Story, M. D.; Song, K.; Raghavan, P.; Timmerman, R.; Chen, B.; Minna, J. D.; Solberg, T. D. *Radiat. Res.* **2010**, *174*, 62−71.
(198) Hong, H.; Zhang, Y.; Severin, G. W.; Yang, Y. N.; Engle, J. W.; Niu, G.; Nickles, R. J.; Chen, X. Y.; Leigh, B. R.; Barnhart, T. E.; Cai, W. B. *Mol. Pharmaceut.* **2012**, *9*, 2339−2349.
(199) Reumann, M. K.; Weiser, M. C.; Mayer-Kuckuk, P. *Trends Biotechnol.* **2010**, *28*, 93−101.
(200) Zhou, Y.; Yan, S. D.; Jia, S. Z.; Wang, H. P.; Fu, Q. X.; Du, J.; Wang, X. H.; Liang, S. Q.; Zhang, J. G.; Zhan, L. S. *Liver Int.* **2012**, *32*, 383−391.
(201) Ploemen, I.; Behet, M.; Nganou-Makamdop, K.; van Gemert, G. J.; Bijker, E.; Hermsen, C.; Sauerwein, R. *Malaria J.* **2011**, *10*, 350.
(202) Hong, H.; Yang, Y. N.; Zhang, Y.; Cai, W. B. *Curr. Pharm. Biotechnol.* **2010**, *11*, 685−692.
(203) Tarantal, A. F.; Lee, C. C. I.; Batchelder, C. A.; Christensen, J. E.; Prater, D.; Cherry, S. R. *Mol. Imaging Biol.* **2012**, *14*, 197−204.
(204) Huang, N. F.; Okogbaa, J.; Babakhanyan, A.; Cooke, J. P. *Theranostics* **2012**, *2*, 346−354.
(205) Gilbert, P. M.; Havenstrite, K. L.; Magnusson, K. E. G.; Sacco, A.; Leonardi, N. A.; Kraft, P.; Nguyen, N. K.; Thrun, S.; Lutolf, M. P.; Blau, H. M. *Science* **2010**, *329*, 1078−1081.
(206) Adler, E. M. *Sci. Signal.* **2012**, *5*, ec97.
(207) Sleeman, J. P.; Nazarenko, I.; Thiele, W. *Int. J. Cancer* **2011**, *128*, 2511−2526.
(208) Blasberg, R.; Piwnica-Worms, D. *Clin. Cancer Res.* **2012**, *18*, 631−637.
(209) David, S.; Carmoy, N.; Resnier, P.; Denis, C.; Misery, L.; Pitard, B.; Benoit, J. P.; Passirani, C.; Montier, T. *Int. J. Pharm.* **2012**, *423*, 108−115.
(210) van der Horst, G.; van Asten, J. J.; Figdor, A.; van den Hoogen, C.; Cheung, H.; Bevers, R. F. M.; Pelger, R. C. M.; van der Pluijm, G. *Eur. Urol.* **2011**, *60*, 337−343.
(211) Inoue, Y.; Sheng, F.; Kiryu, S.; Watanabe, M.; Ratanakanit, H.; Izawa, K.; Tojo, A.; Ohtomo, K. *Mol. Imaging* **2011**, *10*, 377−385.
(212) Wang, W.; Cameron, A. G.; Wendt, J. A.; Mawad, M. E.; Ke, S. *Aust. J. Chem.* **2011**, *64*, 625−632.
(213) Liggett, A.; Crawford, L. J.; Walker, B.; Morris, T. C. M.; Irvine, A. E. *Leukemia Res.* **2010**, *34*, 1403−1409.
(214) Huang, J. G.; Liu, Z. G.; Zeng, W. B. *Anti-Cancer Agents Med. Chem.* **2012**, *12*, 182−186.
(215) Kucherlapati, R. *Clin. Cancer Res.* **2012**, *18*, 625−630.
(216) Arteaga, C. L.; Baselga, J. *Clin. Cancer Res.* **2012**, *18*, 612−618.
(217) de la Zerda, A.; Liu, Z.; Bodapati, S.; Teed, R.; Vaithilingam, S.; Khuri-Yakub, B. T.; Chen, X.; Dai, H.; Gambhir, S. S. *Nano Lett.* **2010**, *10*, 2168−2172.
(218) Kircher, M. F.; de la Zerda, A.; Jokerst, J. V.; Zavaleta, C. L.; Kempen, P. J.; Mittra, E.; Pitter, K.; Huang, R.; Campos, C.; Habte, F.; Sinclair, R.; Brennan, C. W.; Mellinghoff, I. K.; Holland, E. C.; Gambhir, S. S. *Nat. Med.* **1038**, *18*, 829−834.